

# Immunohistochemical techniques for the human inner ear

Ivan A. Lopez<sup>1</sup> · Gail Ishiyama<sup>2</sup> · Seiji Hosokawa<sup>1,3</sup> · Kumiko Hosokawa<sup>1,3</sup> · Dora Acuna<sup>1</sup> · Fred H. Linthicum<sup>1</sup> · Akira Ishiyama<sup>1</sup>

Accepted: 22 July 2016 / Published online: 1 August 2016  
© Springer-Verlag Berlin Heidelberg 2016

**Abstract** In this review, we provide a description of the recent methods used for immunohistochemical staining of the human inner ear using formalin-fixed frozen, paraffin and celloidin-embedded sections. We also show the application of these immunohistochemical methods in auditory and vestibular endorgans microdissected from the human temporal bone. We compare the advantages and disadvantages of immunohistochemistry (IHC) in the different types of embedding media. IHC in frozen and paraffin-embedded sections yields a robust immunoreactive signal. Both frozen and paraffin sections would be the best alternative in the case where celloidin-embedding technique is not available. IHC in whole endorgans yields excellent results and can be used when desiring to detect regional variations of protein expression in the sensory epithelia. One advantage of microdissection is that the tissue is processed immediately and IHC can be made within 1 week of temporal bone collection. A second advantage of microdissection is the excellent preservation of both morphology and antigenicity. Using celloidin-embedded inner ear sections, we were able to detect several antigens by IHC and immunofluorescence using antigen retrieval methods. These techniques, previously applied only in animal models, allow for the study of numerous important proteins expressed in the human

temporal bone potentially opening up a new field for future human inner ear research.

**Keywords** Archival human temporal bone · Microdissection · Paraffin · Cryosections · Immunohistochemistry · Vestibule · Cochlea · Antigen retrieval · Celloidin-embedded sections

## Introduction

The traditional human temporal bone processing at the turn of the twentieth century employed the celloidin-embedding and serial-sectioning methods to evaluate predominantly light microscopic histopathology for clinic–pathologic correlations (Gulya 2007). Earlier studies utilized cytologic descriptions and graphic reconstructions of the cochlea (Guild 1921). Temporal bone science has advanced such that we are now entering a phase of methodological integration, whereby the same temporal bone can be used for light microscopy, transmission electron microscopy (TEM), immunohistochemistry (IHC), non-radioactive in situ hybridization, DNA and proteomics analysis (Aarnisalo et al. 2010; Kong et al. 1998; Merchant et al. 2008; Ishiyama et al. 2009, 2010; Lopez et al. 2005a, b, 2007; Markaryan et al. 2008a, b, c, 2009, 2010a, b; Nguyen et al. 2014; Richard et al. 2015; Schrott-Fischer et al. 1994, 2002a, b, 2007; Wackym et al. 1990). The study of the human inner ear has lagged behind other areas of pathology, in large part due to the inaccessibility of the membranous labyrinth. The temporal bone contains delicate structures, the membranous labyrinth and cochlea, encased in the very dense temporal bone. Furthermore, the tissues are not available for study during a person's lifetime except in specialized cases, such as vestibular endorgans removed by ablative surgery

✉ Akira Ishiyama  
ishiyama@ucla.edu

<sup>1</sup> Head and Neck Surgery Department, David Geffen School of Medicine at UCLA, 951794, 35-64 Rehab, 1000 Veteran Avenue, Los Angeles, CA 90095, USA

<sup>2</sup> Neurology Department, David Geffen School of Medicine at UCLA, 3-250 RNRC, Los Angeles, CA 90095, USA

<sup>3</sup> Otorhinolaryngology/Head and Neck Surgery Department, School of Medicine, Hamamatsu University, 1-20-1 Handayama, Hamamatsu 431-3192, Shizuoka, Japan

in patients diagnosed with intractable Meniere's disease or temporal bone tumors. Thus, there are great technical difficulties in processing the temporal bone in a manner that preserves the morphology while allowing for IHC.

The methodologies used to process human inner ear tissue for IHC and applications have been previously revised by Arnold (1988), Bauwens et al. (1990), Fish et al. (2000), Tian et al. (1999). In the present review, the advantages and disadvantages of the several methodologies available to date to temporal bone investigators for immunohistochemical studies in the human inner ear are discussed. There are two major tissue processing methods available for studies of formalin-fixed postmortem human temporal bones: (1) microdissection of the auditory and vestibular endorgans from temporal bones which yields specimens that can be processed for cryosections, embedded in paraffin or used as whole-mount preparations, and (2) celloidin embedding of temporal bones that have been decalcified, a method that has been widely employed by most archival human temporal bone banks (Schuknecht 1993).

### Microdissected auditory and vestibular endorgans

Formalin-fixed microdissected auditory and vestibular endorgans obtained from human temporal bone specimens have been successfully used to study the immunolocalization of aquaporins, several basement membrane proteins and cochlin in the vestibular endorgans and the cochlea (Lopez et al. 2007; Ishiyama et al. 2009, 2010; Calzada et al. 2012a, b). Using the microdissection technique, the three cristae ampullares, maculae utricle and saccule, as well as the organ of Corti, are removed from the otic capsule of the temporal bone and separately processed for either light or transmission electron microscopic examination (Wright and Meyerhoff 1989).

This technique is advantageous because the dissected tissues can be sectioned serially at any thickness to facilitate detailed cytological examination of specimens, from as thin as 0.1  $\mu$  to as thick as 20  $\mu$ . Another advantage of temporal bone microdissection over celloidin-embedded inner ear tissue is that each dissected endorgan can be properly oriented and processed along the optimal tissue plane, which differs depending on the particular endorgan. Illustrative of this problem (when using the traditional temporal bone processing), only a small fraction (8 %) of the utricle is sectioned in a perpendicular plane, predominantly in the superior pole (Merchant 1999). Thus, by individually dissecting each organ, the specimen can be properly oriented prior to sectioning, allowing accurate cross sectioning perpendicular to the plane for purposes of morphometric studies of specific structures. Previous studies from our laboratory have demonstrated the use of microdissected specimens from postmortem human temporal bones for

design-based stereology (Gopen et al. 2003; Ishiyama et al. 2004; Lopez et al. 2005b).

A third advantage of microdissection is that minimal decalcification is required, allowing for excellent morphological preservation and accurate cytological identification in postmortem specimens. Using the standard procedure for the morphological study of the human temporal bone as established by Schuknecht (1993), the decalcification step for the human temporal bone requires that the specimen remains in ethylenediaminetetraacetic acid (EDTA) for up to 9 months. Temporal bone fixation, microdissection, tissue sectioning and immunostaining can be made within a week. Shorter postmortem times are associated with higher degrees of preservation of the sensory epithelia (se) morphology (Ishiyama et al. 2009). An additional advantage is the ability to apply unbiased stereology in immunostained endorgans (Lopez et al. 2005a). Additionally, it is also possible to use vestibular endorgans microdissected from human temporal bones to extract mRNA to evaluate the expression of muscarinic acetylcholine receptors (Wackym et al. 1996) or mu-opioid receptor mRNA expression by non-radioactive in situ hybridization (Nguyen et al. 2014).

### Formalin-fixed cryostat sections obtained from microdissected endorgans

Formalin-fixed cryostat sections of microdissected vestibular endorgans are routinely used for immunohistochemical studies of the inner ear of numerous animal models. Swartz and Santi (1999) used perilymphatic fixation, decalcification in 10 % EDTA for 3 days, and frozen sections for the study of tenascin-C immunoreactivity (IR) in the chinchilla inner ear. This methodology can also be applied in the human inner ear (Lopez et al. 2005a, 2007; Ishiyama et al. 2009). In the human inner ear, the feasibility and utility of cryosections for IHC have been demonstrated with immunolocalization of several neurotransmitters and peptides (Ishiyama et al. 1994; Kong et al. 1998; Popper et al. 2002), aquaporins (Lopez et al. 2007), basement membrane proteins (Ishiyama et al. 2009) and cochlin (Calzada et al. 2012a, b). Surgically obtained cochlear and vestibular endorgans can also be processed into cryosections and used for IHC (Calzada et al. 2012a, b; Ishiyama et al. 2010; Liu et al. 2009, 2015, 2016; Khalifa et al. 2003). Khalifa et al. (2003) and Rask-Andersen et al. (2000, 2016) used fresh surgically acquired human inner ear specimens to localize several proteins by IHC in the cochlea and spiral ganglia neurons. Of note, the morphological preservation even in postmortem vestibular and auditory endorgans is of sufficient quality to allow for cytological regional identification of IR patterns (Ishiyama et al. 2009). For example, aquaporin 4 is preferentially expressed in the basal portion

of the vestibular supporting cells, while aquaporin 6 is expressed in their apical portion (Lopez et al. 2007).

### IHC in paraffin-embedded sections of the human inner ear

Paraffin-embedded sections of the human inner ear are obtained from formalin-fixed (10–20 %) and decalcified temporal bones or obtained from formalin-fixed microdissected auditory or vestibular endorgans. Once the inner ear tissue is fixed in formalin, dehydrated in ascending ethylic alcohols (30–100 %), cleared with 100 % xylene and embedded in 100 % paraffin, it is possible to obtain 5- to 20- $\mu\text{m}$ -thick sections for IHC.

IHC in paraffin-embedded sections has been conducted in the gerbil cochlea to study the distribution of dystroglycan, an extracellular matrix (ECM) protein, using a combination of microdissection and EDTA (48 h) with excellent morphology and retention of antigenicity (Heaney et al. 2002). Cunningham et al. (2001) described an alternative for IHC of human temporal bones that used a decalcification method with a microwave oven process. A good signal-to-noise ratio of the immunostaining of  $\text{Na}^+\text{K}^+$ -ATPase in the human organ of Corti, as well as acceptable morphological preservation, was demonstrated. Keithley et al. (2000) and Shi et al. (1991, 1992a, b) used paraffin-embedded sections of the human temporal bone and antigen retrieval methodology to localize neurofilaments, peripherin and subunit-1 of cytochrome oxidase (Keithley et al. 1995, 2000, 2001). A modified paraffin-embedding protocol was used for the immunolocalization of prestin and neurofilament antibodies in the human cochlea (Takahashi et al. 2010). Twenty percent formalin was used for fixation, followed by EDTA decalcification for 9 months. Proteinase K (0.2 mg/mL) for 5 min was used for tissue permeabilization. Carbonic anhydrase isoenzyme-IR (Yamashita et al. 1992), laminin-IR (Yamashita et al. 1991) and cytokeratins-IR (Anniko et al. 1989a, b) were detected in paraffin-embedded human fetal inner ear tissue sections. Human temporal bone sections embedded in polyester wax have been used for IHC (Merchant et al. 2006). However, tissue preservation and section quality were suboptimal for histopathology or IHC studies (O'Malley et al. 2009a, b). Thus, paraffin embedding is a good alternative for histology and IHC, when human inner ear tissue embedded in celloidin is not available.

### IHC and IF in whole auditory and vestibular endorgans

Immunostaining of whole endorgans and surface (whole mount) preparations of auditory and vestibular endorgans has widely been used for anatomical and quantitative studies or cell regional distribution (Goran 1968; Rosenhall

1972; Rosenhall and Rubin 1975). Histochemical staining of actin with fluorescence-labeled phalloidin has been used to identify vestibular and auditory hair cell stereocilia and the apical portion of supporting cells. Whole endorgan staining of nerve fibers has been possible using antibodies against neurofilaments and markers that identify specific neuronal populations, i.e., calbindin, calretinin or nerve terminals, i.e., synaptophysin (Nadol et al. 1993). The organization of nerve terminals in the human cochlea was recently investigated using antibodies against several proteins present in the synaptic terminals (Viana et al. 2015): CTBP2 (to identify synaptic ribbons), anti-neurofilaments (nerve axons), anti-myosin VIIa (hair cell identification) and choline acetyltransferase to identify efferent axons. Viana et al. (2015) used triple and quadruple-IF staining to reveal the pattern of afferent and efferent innervation in human postmortem material and showed evidence that cochlear synaptopathy in the absence of hair cells loss may be an important factor in human presbycusis.

The whole immunostained endorgan has been embedded in plastic to obtain thin sections (0.5–1  $\mu\text{m}$ ) and also has been used for design-based unbiased stereology (Lopez et al. 2005a). Whole-mount immunostained specimens have also been used to conduct TEM (Nadol et al. 1993; McCall et al. 2009; Taylor et al. 2015).

### IHC in celloidin-embedded sections

A large number of archival human temporal bone specimens collected over the past 85 years are available in the USA and Europe for histopathological studies of the auditory and vestibular system (Schuknecht 1993; Merchant et al. 1993, 2008). Currently there are only three active temporal bone laboratories in the USA that continue to embed human inner ear tissue in celloidin (Chole 2010). The traditional method of temporal bone processing uses formalin as fixative (10 %, neutral-buffered formalin). Before decalcification, the temporal bones (immersed in formalin) are stored in a cold room or at 4 °C in the refrigerator, for 1–3 weeks. Decalcification step with EDTA (0.27–0.48 M, with or without 1 % formalin, pH 7.2–7.3) takes up to 9 months. Temporal bone specimens are then dehydrated in graded ascending ethylic alcohol and embedded in celloidin over a 3-month period. Detailed procedures of temporal bone collection, fixation, decalcification and celloidin embedding were described by Merchant (2010). Horizontal sections of celloidin-embedded temporal bones are obtained with a sliding microtome. The specimens are serially sectioned at 20  $\mu\text{m}$ , and every tenth section is stained with hematoxylin and eosin. The celloidin-embedding method yields superb morphological and histopathological preservation of the human inner ear that can be used for IHC (Ganbo et al. 1997, 1999; Cunningham

et al. 2001; Keithley et al. 1994, 2000; Markaryan et al. 2011; Ying and Balaban 2009; Ahmed et al. 2013; Balaker et al. 2013; Nguyen et al. 2014; Vorasubin et al. 2016). It is important to have in consideration the length of fixation specially for IHC. Excessive cross-link of proteins by the fixative will affect the binding of the antibody. Antigen retrieval steps discussed in this review can help to restore immunogenicity.

Several laboratories have described methods for celloidin removal and antigen retrieval steps for IHC (Shi et al. 1992a, b, 1993, 1998; O'Malley et al. 2009a). These two steps are necessary to expose the antigens and allow primary antibody binding. Antigen retrieval technique was first described by Battifora and Kopinski (1986) and was designed to increase epitope antigenicity for immunohistochemical studies. Once celloidin is completely removed from the tissue section, it is immersed in a heavy metal solution and heating in the microwave oven (Shi et al. 1992a, b, Appendix). The result is a significant increase in antigenicity and binding of proteins (O'Rourke and Padula 2016).

Thick celloidin-embedded sections (20–30  $\mu\text{m}$ ) of single temporal bone are kept immersed in 80 % ethylic alcohol for subsequent histological and/or immunohistochemical analysis including proteomics (Tian et al. 1999; Aarnisalo et al. 2010; Markaryan et al. 2010a, b). Cytologic quantification of the cochlea is feasible when postmortem time is sufficiently short (Schuknecht 1993). Detailed techniques for celloidin removal from temporal bone sections have been described in detail (O'Malley et al. 2009a). O'Malley et al. (2009a, b) used clove oil, acetone, ether-alcohol and methanol saturated with sodium hydroxide. The first three substances resulted in incomplete removal of celloidin, affecting the quality of immunostaining. Methanol–sodium hydroxide method completely removed celloidin and produced good immunostaining with six antibodies: prostaglandin D synthase,  $\text{Na}^+\text{K}^+\text{-ATPase}$ , aquaporin 1, connective tissue growth factor, tubulin and 200kd neurofilaments. We used sodium ethoxide to remove celloidin from the sections and obtain very good immunoreactive signal with almost no background (Calzada et al. 2012a, b; Ahmed et al. 2013; Balaker et al. 2013; Nguyen et al. 2014; Vorasubin et al. 2016).

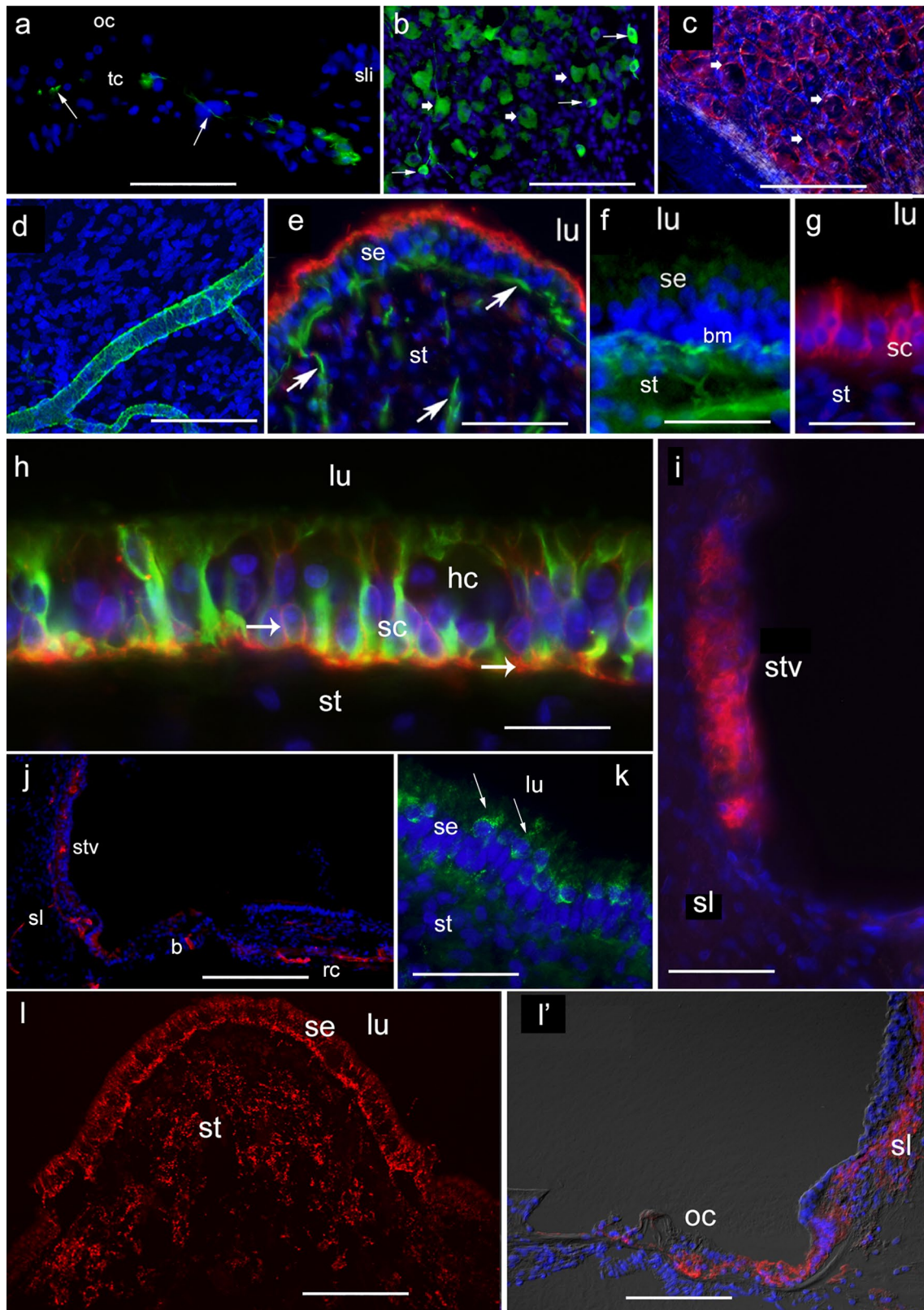
In this review, we describe the current protocols for IHC using formalin-fixed frozen, paraffin-embedded and celloidin-embedded tissue sections of the human inner ear. The three types of tissue processing are useful for the identification of different types of antigens by IHC. We then contrast the advantages and disadvantages of these methodologies. Details of the various protocols used in this review are presented in “Appendix” section. IHC staining and IF staining in human inner ear tissue using these protocols are described below.

**Fig. 1** Immunofluorescence (IF) staining in frozen sections obtained from microdissected auditory and vestibular endorgans. **a** Neurofilaments-IF in the organ of Corti (*oc*). *Arrows* point to IF terminals and fibers. Tunnel of Corti (*tc*), spiral limbus (*sl*), lumen (*lu*). **b** Neurofilament-IF in the spiral ganglia neurons *arrows* point to IF large-size spiral ganglia neurons, *thick arrowhead* point to IF small-size spiral ganglia neurons. **c**  $\text{Na}^+\text{K}^+\text{-ATPase}$ -IF in satellite cells (*arrowheads*) that surround spiral ganglia neurons. **d** Smooth muscle actin-IF in a blood vessel of the modiolus. **e** Neurofilament-IF in nerve fibers located in the crista stroma (*st*) and underneath the sensory epithelia (*se*) (*green color, arrows*), phalloidin staining (*red*) at the apical portion of the sensory epithelia. **f** Collagen IV-IF in basement membrane (*bm*) of the utricle stroma. **g** Cx-26-IF in supporting cells (*sc*) of the utricle sensory epithelia. **h** Aquaporin-4-IF (*red*) and GFAP-IF (*green*) in the cytoplasm of supporting cells (*sc*) of the utricle sensory epithelia. Hair cells (*hc*) were non-IF. *Arrows* point to AQP4-IF (*red*) at the basolateral portion of the *sc*. **i** Kir 4.1-IR in the stria vascularis (*stv*) of the cochlea, spiral ligament (*sl*). **j** WARP-IF in blood vessels of the stria vascularis (*stv*), spiral ligament (*sl*), basilar membrane (*b*), Rosenthal's canal (*rc*). **k** Cytochrome-C-IF in hair cells (*arrows*) of the sensory epithelia (*se*). **l** Cx30-IF in the crista ampullares sensory epithelia (*se*) and stroma (*st*) (*red punctate*) and **l'** the cochlea, *red punctate* in the organ of Corti (*oc*), spiral ligament (*sl*). DAPI in *blue color* shows staining in cell nuclei. Magnification *bars a* 150  $\mu\text{m}$ , **b** 125  $\mu\text{m}$ , **c** 125  $\mu\text{m}$ , **d** 50  $\mu\text{m}$ , **e** 70  $\mu\text{m}$ , **f** 50  $\mu\text{m}$ , **g** 50  $\mu\text{m}$ , **h** 25  $\mu\text{m}$ , **i** 80  $\mu\text{m}$ , **j** 200  $\mu\text{m}$ , **k** 50  $\mu\text{m}$ , **l** 125  $\mu\text{m}$ , **l'** 125  $\mu\text{m}$

## IHC in microdissected audio-vestibular endorgans

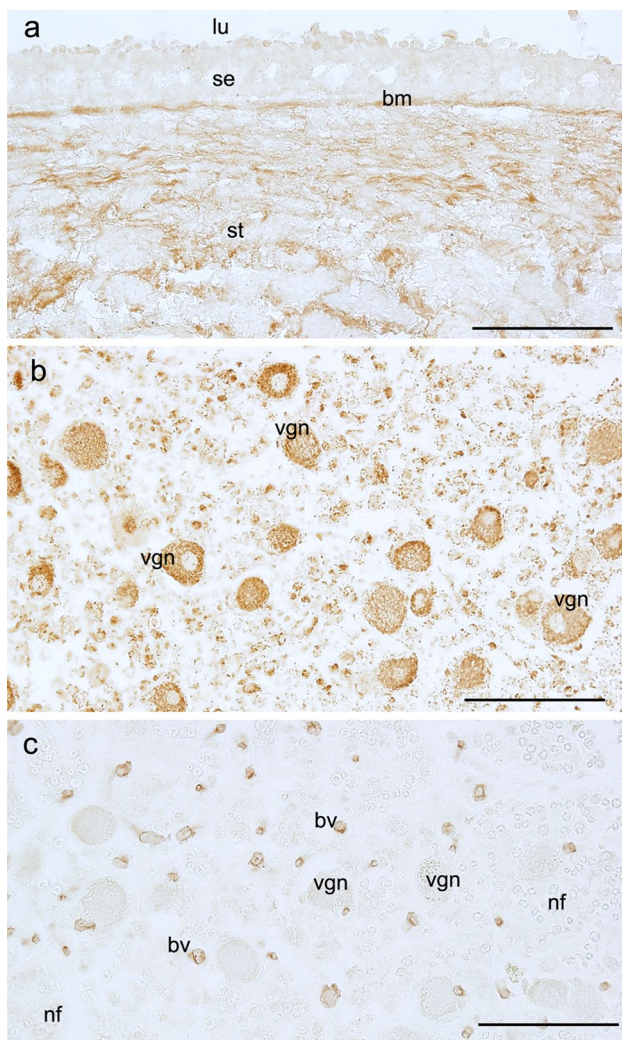
### Formalin-fixed cryostat sections

Figure 1 shows immunofluorescence (IF) micrographs using formalin-fixed frozen sections obtained from microdissected auditory and vestibular endorgans harvested from postmortem temporal bones. A wide variety of intracellular and extracellular proteins were detected using this protocol (“Appendix” section). IF of cryostat sections of the cochlea using neurofilaments antibodies demonstrated sensitivity to detect nerve fibers running throughout the modiolus, reaching the base of the inner and outer cochlear hair cells (Fig. 1a). Neurofilament-IF was also seen the soma of spiral ganglia neurons (Fig. 1b). Satellite cells that surround spiral ganglia neurons were  $\text{Na}^+\text{K}^+\text{-ATPase}$ -IF (Fig. 1c). Blood vessels within the cochlea were identified with the use of antibodies against alpha-smooth muscle actin (Fig. 1d). In the crista ampullaris, neurofilament-IF identified nerve fibers of varied diameter within the stroma and running throughout the sensory epithelium. Phalloidin-rhodamine visualized the apical portion of supporting cells and hair cells stereocilia (Fig. 1e). In the macula utricle, antibodies against collagen IV identified the perineural basement membrane associated with nerve fibers that run within the stroma and also delineated the basement membrane underneath the *se* (Fig. 1f). Connexin (Cx)-26-IF was localized in the supporting cells of the macula utricle (Fig. 1g). Figure 1h shows aquaporin-4-IF (red color) and GFAP-IF (green color) in the supporting



cells of the macula utricule se. IF for the inward rectifier  $K^+$  channel 4.1 was detected in the stria vascularis of the cochlea (Fig. 1i). von Willebrand A domain-related

protein (WARP)-IF was detected in small- and large-size blood vessels of the cochlea (Fig. 1j). Figure 1k shows cytochrome-C-IF in the hair cells cytoplasm. Cx-30-IF



**Fig. 2** Immunohistochemical staining in paraffin sections obtained from microdissected endorgans. **a** Cochlin-IR in a cross section of the macula utricule. Cochlin-IR was seen in the basement membrane (*bm*) of the sensory epithelia and extracellular matrix of the stroma (*st*). The sensory epithelium (*se*) was non-IR. **b** Superoxide dismutase-2 (SOD-2)-IR in the cytoplasm of the vestibular ganglia neurons (*vgn*). **c** WARP-IR in a section of the vestibular ganglia. WARP-IR was located in blood vessels (*bv*). Vestibular ganglia neurons (*vgn*) and nerve fibers (*nf*) were non-IR. Bar 100  $\mu$ m in every figure

was seen in the *se* of the crista ampullares (Fig. 11) and cochlea (Fig. 11').

#### Paraffin-embedded tissue sections

Figure 2 shows IHC staining in paraffin-embedded tissue sections of microdissected macula utricule and vestibular ganglia. Figure 2a shows cochlin-IR in a cross section of the macula utricule. Cochlin-IR was seen in the basement membrane of the *se* and ECM of the stroma. The *se* was non-IR. Figure 2b shows superoxide dismutase-2 (SOD-2)-IR in a cross section of the vestibular ganglia. SOD-2-IR

was seen in the cytoplasm of the vestibular ganglia neurons (punctated distribution resembling mitochondria). Figure 2c shows WARP-IR in a consecutive section of the vestibular ganglia. WARP-IR was confined to the blood vessels. Vestibular ganglia neurons and nerve fibers were non-IR. Paraffin-embedded microdissected specimens yielded good IHC, and numerous antibodies have been tested using this type of tissue sections (Table 1).

#### Immunofluorescence in whole auditory and vestibular endorgans

Figure 3a–c shows a whole-mount preparation of the organ of Corti immunostained with antibodies against myosin VIIa to visualize outer and inner hair cells. Figure 3a shows a low magnification view from the mid-apical organ of Corti. Higher magnification demonstrates myosin VIIa-IF in the hair cells (Fig. 3b in red color). Simultaneous visualization with  $\text{Na}^+$ ,  $\text{K}^+$ -ATPase antibodies shows IF in the inner and outer sulcus cells (Fig. 3b in green color). In another specimen, hair cells and their stereocilia were identified with myosin VIIa antibodies and phalloidin Oregon green (Fig. 3c, red and green color, respectively). Actin was seen at the junctional complexes along the circumference of supporting cells. Figure 3d shows neurofilament-IF in nerve fibers of the cochlea from the hook region to the apical portion. Figure 3e shows a higher magnification view from the apical portion from Fig. 3d. Immunofluorescent nerve fiber processes that course radially toward the organ of Corti were easily identified. Figure 3f shows a whole-mount preparation of the saccule subjected to IF staining with antibodies against calmodulin. Vestibular hair cells were well visualized (Fig. 3f). Neurofilaments-IF identified nerve fibers and terminals in a whole-mount preparation of the utricule (Fig. 3g). Figure 3h shows another macula utricule stained by double labeling with calmodulin and neurofilaments antibodies that identify hair cells and the innervating vestibular nerve fibers, respectively.

#### IHC in celloidin-embedded tissue sections

Using the IHC protocol for celloidin-embedded sections (“Appendix” section), we were able to localize several proteins in the human inner ear. Figure 4a–b'' shows  $\beta$ 2-laminin-IR and collagen IV-IR in the cochlea and vestibular endorgans. These celloidin-embedded immunostained sections were counterstained with hematoxylin (purple color). In the cochlea,  $\beta$ 2-laminin-IR (dark amber color) was found in perivascular basement membranes. Reissner’s membrane was also  $\beta$ 2-laminin-IR, while the tectorial membrane was negative (Fig. 4a). Of note, Reissner’s membrane and the tectorial membrane morphology were well preserved. Figure 4a' shows the  $\beta$ 2-laminin-IR

**Table 1** Summary of proteins detected by IHC and IF in the human inner ear

Antibody tested	Cryostat (microdissected)	Paraffin	Celloidin	References
Neurofilaments	+	+	+	1, 15
Myosin VII	+	–	–	1
Phalloidin	+	–	–	1
GFAP	+	NR	–	1, 2, 3
Kir4.1	+	NR	NR	1
Connexin 26	+	NR	+	1, 14, 21
Connexin 30	+	NR	–	1
Col IV	+	NR	+	1, 2, 8
Nidogen	+	NR	–	2
$\beta$ -Laminin	+	+	+	1, 2, 17
$\alpha$ -Dystroglycan	+	NR	NR	1
Tenascin-C	+	NR	–	2
Aquaporin 1	+	NR	–	1, 3
Aquaporin 4	+	NR	–	2, 3
Aquaporin 6	+	NR	NR	3
SOD-2	+	+	+	1, 7
Cytochrome-C	+	+	+	1
Cochlin	+	+	+	1, 5
$\text{Na}^+\text{K}^+$ -ATPase	+	+	+	1, 12, 21
VWA	+	+	+	1, 6
Choline acetyltransferase	+	+	NR	9, 13, 16
GABA	+	NR	NR	23
Synaptophysin	+	+	+	1, 3, 4, 11
S-100	NR	+	+	10, 19, 21
Carbonic anhydrase	NR	+	+	18, 21
Calmodulin	+	NR	NR	1
Smooth muscle actin	+	+	NR	1, 6
Vimentin	+	NR	NR	3
Cytokeratin	NR	+	NR	20
Cytochrome oxidase	NR	NR	+	22, 24
GLAST	+	–	+	25
TOM-20	+	NR	+	26
Mu-opioid receptor	–	NR	+	27
Neuroglobin	–	NR	+	28
Prestin	–	+	+	1, 15
Acetylated tubulin	+	–	+	1

(1) Present study, (2) Ishiyama et al. (2009), (3) Lopez et al. (2007), (4) Nadol et al. (1993), (5) Robertson et al. (2006), (6) Duong et al. (2011), (7) Ying and Balaban (2009), (8) Markaryan et al. (2009), (9) Ishiyama et al. (1994), (10) Anniko et al. (1989a), (11) Khalifa et al. (2003), (12) Keithley et al. (1995), (13) Schrott-Fischer et al. (1994), (14) Liu et al. (2009), (15) Takahashi et al. (2010), (16) Popper et al. (2002), (17) Yamashita et al. (1991), (18) Yamashita et al. (1992), (19) Shi et al. (1992a, b), (20) Anniko et al. (1989b), (21) Doherty and Linthicum (2004), (22) Keithley et al. (2001), (23) Kong et al. (1998), (24) Markaryan et al. (2008c), (25) Ahmed et al. (2013), (26) Balaker et al. (2013), (27) Nguyen et al. (2014), (28) Vorasubin et al. (2016)

+ Tested and detected by IHC or IF (present study), – not detected in the present study, NR not reported

around the stria vascularis blood vessels. This celloidin section was not counterstained with hematoxylin to demonstrate the specific  $\beta$ 2-laminin-IR and the lack of background. Figure 4a'' shows perivascular  $\beta$ 2-laminin-IR in the spiral ganglia from another temporal bone celloidin

section. Figure 4a''' shows  $\beta$ 2-laminin-IR in the basement membrane of the se of the saccular macula. Perivascular  $\beta$ 2-laminin-IR was seen around blood vessels within the stroma. Figure 4b shows collagen IV-IR in the vasculature of the spiral ligament and spiral prominence. Figure 4b'

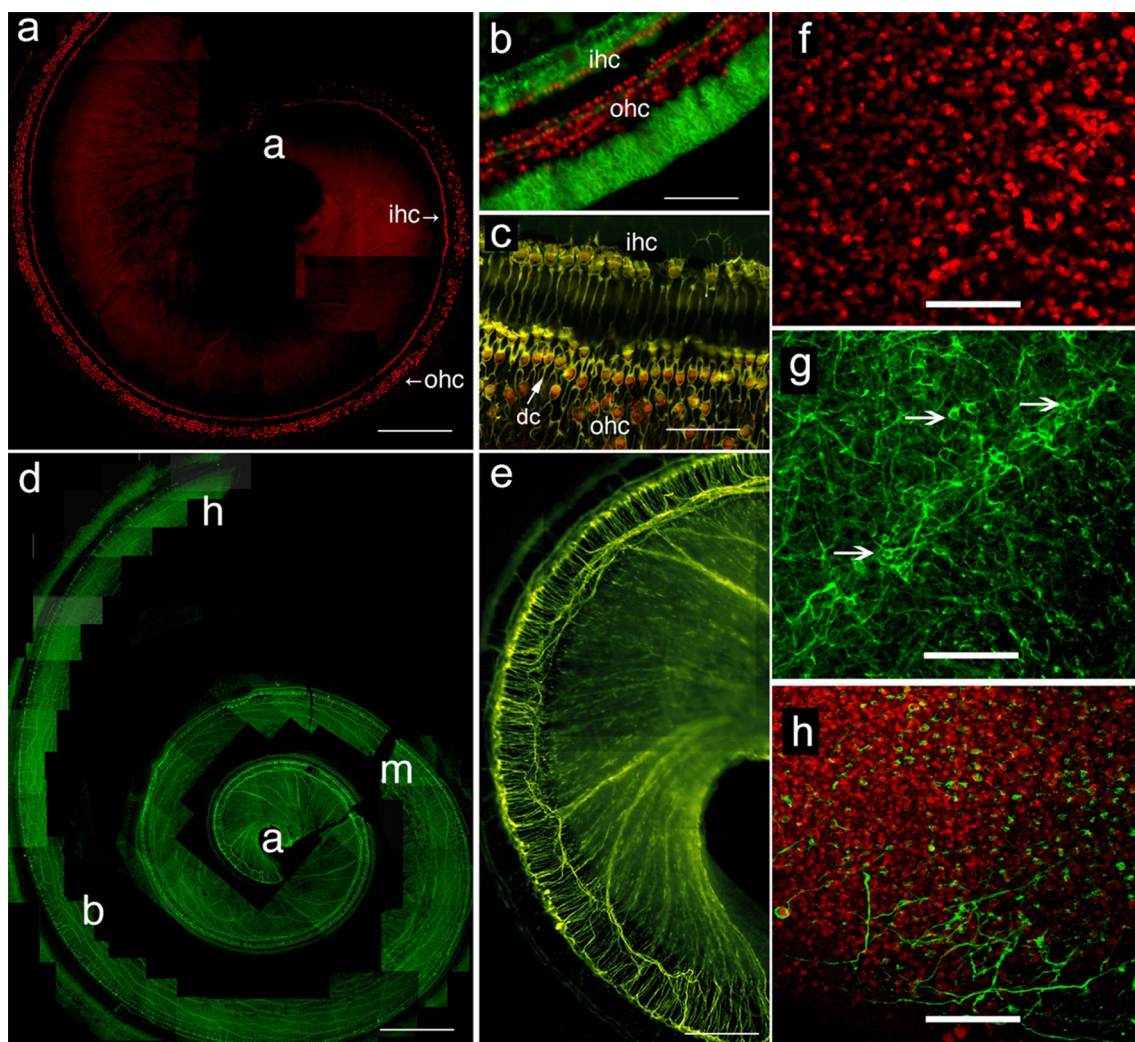


**Fig. 3** Immunofluorescence staining in whole-mount preparations. **a** Myosin VIIa in the mid-apical portion of the cochlea. Inner hair cells (*ihc*) and outer hair cells (*ohc*) were IF to myosin VIIa (*red*). **b** Double immunolabeling of myosin VIIa (*red*) and  $\text{Na}^+\text{K}^+\text{ATPase}$  (*green*). **c** The organ of Corti showing phalloidin Oregon green staining in the inner (*ihc*) and outer (*ohc*) hair cells stereocilia and the apical portion of Deiter's cells (*dc*). Myosin VIIa-IF (*red*) was seen in the hair cell cytoplasm. **d** Neurofilament-IF in the whole cochlea, apical (*a*),

middle (*m*), basal (*b*), hook region (*h*). **e** Higher magnification view of the apical portion of the cochlea in **d**. **f** Calmodulin-IF in hair cells of the macula saccule. **g** Neurofilament-IF in fibers of the macula utricle. Thick nerve fibers and calyceal terminals (*arrows*) are clearly identified. **h** Double labeling of myosin VIIa (*red*) and neurofilaments (*green*). Magnification bars **a** 400  $\mu\text{m}$ , **b** 150  $\mu\text{m}$ , **c** 50  $\mu\text{m}$ , **d** 250  $\mu\text{m}$ , **e** 100  $\mu\text{m}$ , **f**, **g** 100  $\mu\text{m}$ , **h** 150  $\mu\text{m}$

shows collagen IV-IR in the basement membrane of the organ of Corti and in the spiral limbus. Figure 4b'' shows collagen IV-IR around the spiral ganglia neurons. Figure 4c, d shows SOD-2-IR and NF-IR in the cytoplasm of spiral ganglia neurons. Figure 4e shows acetylated tubulin-IR in pillar and Deiter's cells of the organ of Corti.

#### Immunofluorescence in celloidin-embedded tissue sections

Colocalization of prestin and acetylated tubulin identifies outer hair cells (green) and supporting cells (red),

respectively (Fig. 5a); it was possible in celloidin-embedded sections of the human cochlea. DAPI in blue color allows the identification of cell nuclei. Laser confocal microscopy was feasible in this type of tissue, with superb signal-to-noise ratio. Figure 5b shows a stack of images (0.5  $\mu\text{m}$ ) obtained with the confocal microscope; the creation of this stack using ImageJ (public software) allows the 3D view of hair cells (green) and supporting cells (red) with prestin and acetylated tubulin antibodies, respectively. DAPI (blue) stain allows the identification of cell nuclei (Fig. 5b). The exposure of celloidin-embedded sections to UV light before IF quenches autofluorescence effectively ("Appendix" section).



## Discussion

In this review, we show the results from the application of IHC using formalin-fixed frozen and paraffin sections obtained from microdissected human auditory and vestibular endorgans. Both tissue processing methods demonstrated excellent preservation of antigenicity and morphology. Whole mount (surface preparations) of the cochlea and vestibular endorgans was also useful to detect regional expression of several proteins. IHC and IF were also successfully performed in celloidin-embedded sections. The advantages and disadvantages for each type of tissue processing methods are discussed below.

### IHC in microdissected audio-vestibular endorgans

#### *Advantages*

The use of cryostat sections obtained from microdissected auditory and vestibular endorgans for IHC has several advantages. Each endorgan can be properly oriented and thin sections can be obtained. Processing of microdissected specimens has a much shorter time requirement compared to the preparation of celloidin-embedded specimens. Since little or no decalcification is needed, fixation and tissue sectioning can be as short as 1 week. For the cochlea, it is recommended to remove as much connective tissue and surrounding bone as possible and then place the otic capsule containing the cochlea into EDTA for 3 weeks. The tissue embedding media (i.e., Tissue Tek) used to obtain cryostat sections are soluble to water, and it is easily removed before IHC or IF.

One major advantage of formalin-fixed frozen sections of the cochlea or vestibule is the possibility of multi-screening of several antigens using double or triple labeling (Table 1). The use of multiple cellular markers allows the study of multiple specific proteins in the normal and pathological inner ear. Formalin-fixed human and animal inner ear frozen sections can be used as a positive control to test antibodies in cases where paraffin or celloidin sections do not show the expected protein expression. Normative tissue when collected within 3- to 6-h postmortem can be used to compare immunostaining with pathological tissue obtained from ablative surgery (i.e., labyrinthectomy). Formalin-fixed frozen sections are also a good reference for testing labile antigens to be investigated in valuable celloidin-embedded tissue sections. As revised by Shi et al. (1998) for any antibody tested, knowledge of immunolocalization of the antigen in formalin-fixed frozen fresh tissue is valuable as a gold standard. Otherwise, frozen tissue sections should be stained simultaneously with paraffin or celloidin sections to validate IHC or IF methods.

We have previously reported that microdissected vestibular endorgans can be used for stereology quantification (Gopen et al. 2003; Ishiyama et al. 2004; Lopez et al. 2005a). Microdissected crista ampullaris or utricle were subjected to whole-mount IHC as described on whole-mount methods (“Appendix” section), and then, the immunoreacted vestibular endorgans were immediately dehydrated, properly oriented (in the desired plane) and embedded in plastic. Two-micron-thick serial sections of the whole organ were obtained and counterstained with toluidine blue. Design-based stereology was then applied (Lopez et al. 2005a). We have also used formalin-fixed microdissected vestibular endorgans embedded in paraffin for molecular biological studies (Pegadar et al. 2006). Other laboratories have used this type of tissue processing for proteomics (Robertson et al. 2006). Using a similar methodology, aquaporin 1, 4 and 6 (Lopez et al. 2007; Ishiyama et al. 2010), collagen IV, nidogen,  $\beta$ -laminin,  $\alpha$ -dystroglycan and tenascin-C (Ishiyama et al. 2009) were detected in cryostat sections of microdissected auditory and vestibular endorgans. More recently, we have been able to implement non-radioactive *in situ hybridization protocols* to investigate the mRNA expression of the mu-opioid receptor in formalin-fixed cryostat sections of the human cochlea and protein localization by IHC using celloidin-embedded tissue sections (Nguyen et al. 2014).

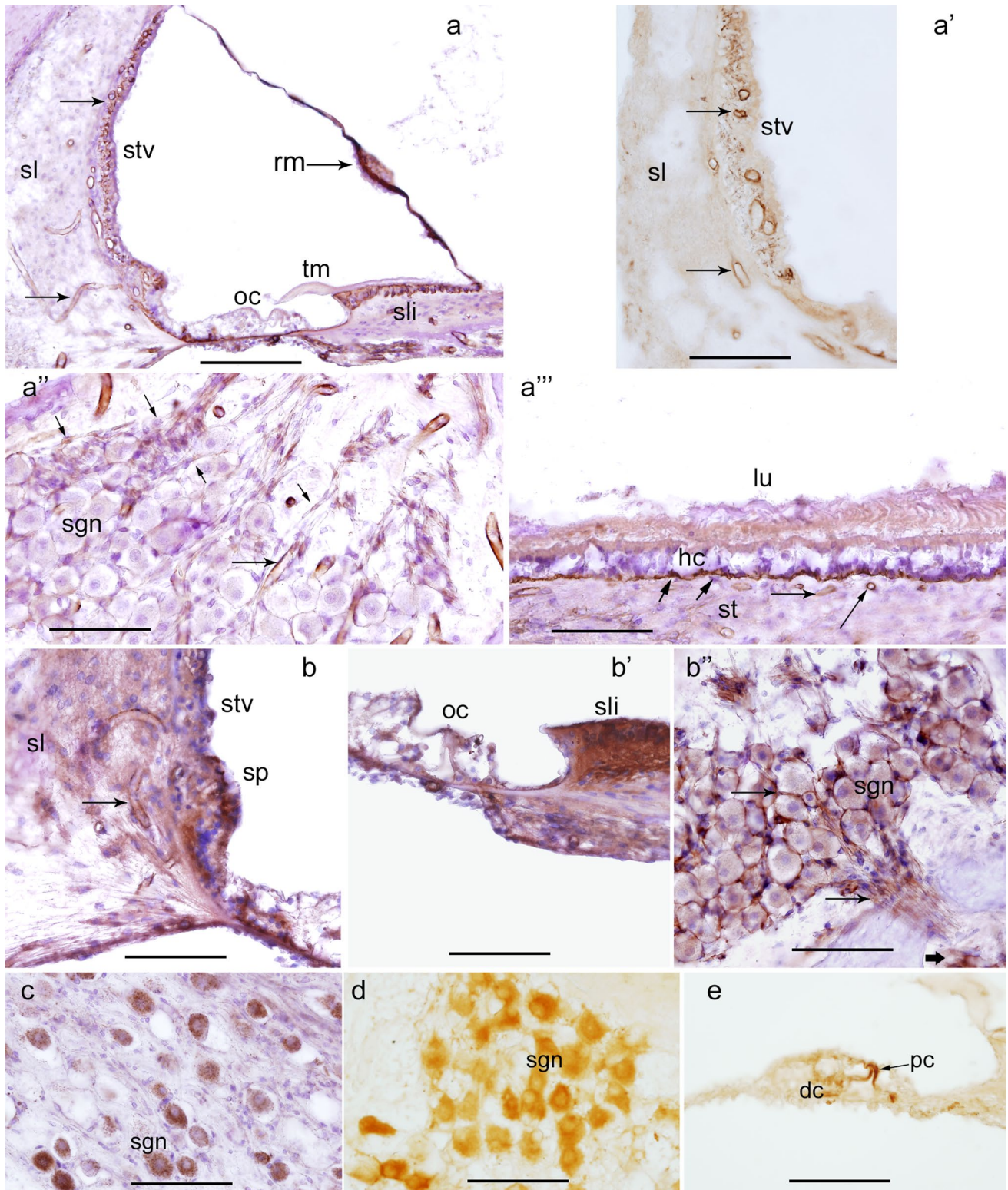
#### *Disadvantages*

Some structures are lost during auditory and vestibular endorgan microdissection, for example the tectorial and Reissner’s membrane, the endolymphatic sac and the labyrinth membrane that surrounds the vestibular endorgans. Storage of the cryosections requires an ultra-low temperature refrigerator (−80 °C) and the need of a backup system. The quality of staining may decrease by prolonged storage of the sections. However, uncut tissue can be kept frozen. Training is required to learn the audio-vestibular endorgan microdissection. Antigen retrieval treatment may need to be applied to the formalin-fixed frozen sections in the case of antigens sensitive to formalin fixation. The microwave heating treatment may affect the integrity of the fragile tissue attached to the glass slide.

### IHC in whole endorgans

#### *Advantages*

One of the advantages of whole-mount (surface preparations) specimens is that regional distribution of expression of antigens can be investigated. Whole-mount preparations



are especially useful in the cochlea where there is standardization of regional classification and known differential expression of proteins regionally based. Whole-mount preparation is an ideal preparation for confocal studies

(Viana et al. 2015). Whole endorgans can be embedded in plastic after IHC or IF and image documentation. Thin plastic serial sections can be used for unbiased stereology and quantification (Lopez et al. 2005a). Nadol et al. (1993)

◀ **Fig. 4** IHC in celloidin-embedded sections. **a**  $\beta$ 2-Laminin-IR within basement, vascular (*arrows*) and perineural membranes (*dark amber color*) in the stria vascularis (*stv*), spiral ligament (*sl*), organ of Corti (*oc*), Reissner's membrane (*rm*), spiral limbus (*sli*), and the basilar membrane. The tectorial membrane (*tm*) was non-IR. **a'**  $\beta$ 2-Laminin-IR in perivascular basement membrane of the spiral ligament (*sl*) and stria vascularis (*stv*) (*arrows*). **a''**  $\beta$ 2-Laminin-IR in perivascular (*long arrows*) and perineural (*short arrows*) basement membranes of the spiral ganglia. Spiral ganglia neurons (*sgn*). **a'''**  $\beta$ 2-Laminin-IR in the basement membrane underneath the sensory epithelia (*short arrows*) and also perivascular (*long arrows*) basement membranes, hair cells (*hc*), lumen (*lu*). **b** Collagen IV-IR in stria vascularis (*stv*) and spiral ligament (*sl*) perivascular basement membranes (*arrows*), spiral prominence is also collagen IV-IR (*sp*). **b'** Collagen IV-IR was seen at the spiral limbus (*sli*), organ of Corti (*oc*). **b''** Collagen IV-IR in perineural (*short arrow*) and perivascular (*arrows*) basement membrane of the spiral ganglia. Spiral ganglia neurons (*sgn*). **c** SOD2-IR in the spiral ganglia neurons (*sgn*). **d** Neurofilaments-IR in the spiral ganglia neurons (*sgn*). **e** Acetylated tubulin-IR in the pillar cells (*pc*), and Deiter's cells. **e** Celloidin-embedded tissue sections counterstained with hematoxylin (except for **a'**, **d**, **e**). Magnification bars **a** 200  $\mu$ m, **a'** 100  $\mu$ m, **a''** 100  $\mu$ m, **a'''** 100  $\mu$ m, **b** 75  $\mu$ m, **b'** 75  $\mu$ m, **b''** 120  $\mu$ m, **c**, **d** 150  $\mu$ m, **e** 40  $\mu$ m

used microdissection and preembedding immunostaining and TEM to visualize synaptophysin.

#### Disadvantages

Penetration of the reagents (PBS, blocking solution), including the antibody of interest, can be a problem, especially with respect to the crista ampullaris. This is notable in the identification of mesenchymal cells and the relative diminished penetration into the basal portion of supporting cells. For vestibular endorgans, the penetration of reagents

and antibodies is limited to 5–10  $\mu$  in the epithelial portion, and the compactness of the stromal tissue underneath the se can be a limiting factor for access of antibodies. Increasing the concentration of Triton-X100 can allow for increased permeabilization of the tissue.

#### IHC in paraffin sections

##### Advantages

There are several advantages of the paraffin-embedded method. Paraffin embedding requires minimum equipment, and most of the equipment is standard in a traditional histopathology laboratory. Additionally, paraffin-embedding process is relatively quick and requires relatively less training than celloidin embedding and sectioning. Tissue samples embedded in paraffin can be used many years after they were obtained and can be kept as a paraffin tissue bank. Paraffin-embedded tissue sections are resistant to microwave oven heating during the antigen retrieval method.

IHC in paraffin-embedded tissues is used routinely for pathological specimens, and numerous antibodies can be tested for diagnostic purposes. In some cases, the antibodies are specifically designed to identify antigens in formalin-fixed paraffin-embedded specimens. Indirect IHC methods or fluorescence-labeled secondary antibodies can be used in this type of tissue. In Zehnder et al. (2005), a mid-modiolar section was stained with hematoxylin and eosin, and the remaining sections were used for IHC of  $\alpha$ 2,  $\alpha$ 3 and  $\alpha$ 5 collagen IV in Alport syndrome. The temporal bones had been in formalin for several years prior to

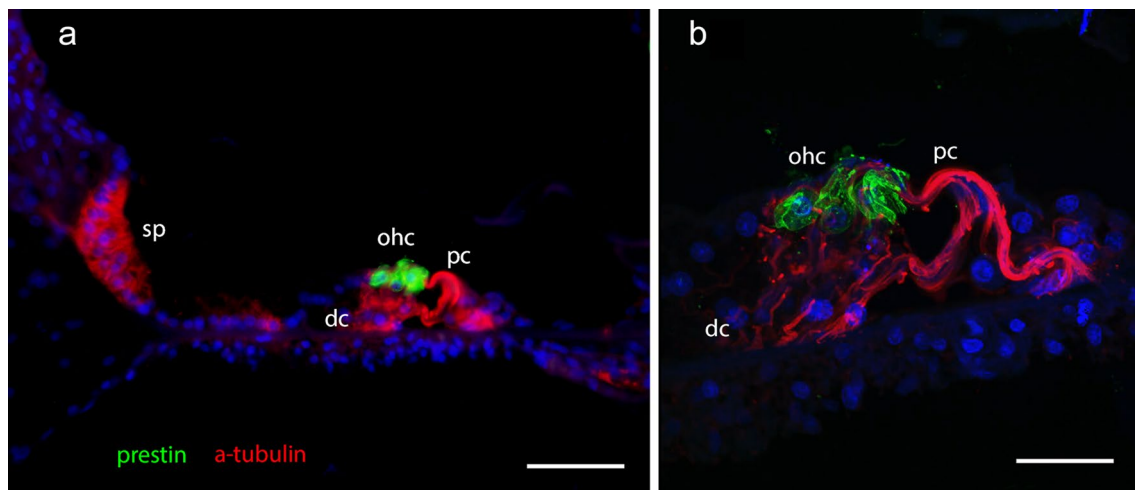


**Fig. 5** Immunofluorescence staining of prestin and acetylated (a)-tubulin in the organ of Corti. Celloidin-embedded section. **a** Prestin-IF (*green*) was seen in outer hair cells (*ohc*), acetylated tubulin (*red*) was seen in pillar cells (*pc*), Deiter's cells (*dc*) and the cells of the spiral prominence (*sp*). Photomicrograph obtained with a fluores-

cent microscope. **b** Photomicrograph obtained with a laser confocal microscope as in (**a**) higher magnification, prestin-IF was localized in outer hair cells (*green*), acetylated tubulin-IF identified in the Deiter's cells (*dc*) and pillar cells (*pc*) (*red*). Magnification bars **a** 70  $\mu$ m, **b** 15  $\mu$ m

processing. Paraffin-embedded human temporal bone specimens were also used to conduct proteomics and IHC for cochlin expression (Robertson et al. 2006). In that study, the temporal bones had been in 10 % formalin for several years and then later decalcified in EDTA and embedded in paraffin. Eight-micron sections were made and immunostained in the traditional manner.

#### *Disadvantages*

Alcohols and xylenes are used for dehydration and paraffin infiltration, and heating (55–60 °C) may affect antigen conformation. Also, the degree of shrinkage is high in paraffin-embedded tissue (from 30 to 40 %). This shrinkage produces alterations of the tissue (Tang and Nyengaard 1997; Philipp and Ochs 2013), specially in the delicate cochlea and vestibular endorgans. The preservation of delicate structures like the Reissner's membrane and the tectorial membrane is not feasible. The use of paraffin-embedded tissue for quantitative unbiased stereology is not recommended as the cutting process can cause tissue loss, e.g., lost caps (physical removal of nucleolar fragments by the cutting blade). Finally, paraffin must be completely removed from the tissue to avoid false-positive reactions.

#### **IHC in celloidin-embedded sections**

##### *Advantages*

Most of the human temporal bone banks have a collection of hematoxylin and eosin sections, from which there are remaining 9 out of 10 sections unstained that can be used for different types of staining, including IHC, histochemistry, molecular biology or proteomics (Jokay et al. 1998; Kammen-Jolly et al. 2001; Khetarpal 2000; Robertson et al. 2001, 2006; Merchant et al. 2008; Aarnisalo et al. 2010; Markaryan et al. 2008a, b, c, 2009, 2010a, b, 2011; Maekawa et al. 2010; Nelson and Hinojosa 2014). The tectorial membrane and Reissner's membrane are generally well preserved, which often is not the case in paraffin-embedded or microdissected specimens. Celloidin-embedding process causes minimum shrinkage of the tissue (Gardella et al. 2003). Another major advantage is the availability of panoramic views of the inner ear. For example, mid-modiolar temporal bone sections include the cochlea and vestibule, as well as the surrounding and supporting structures, i.e., middle ear, vasculature as well as neuronal components (spiral and vestibular ganglia as well as nerve fibers), and the endolymphatic sac. This allows for the localization of the different inner ear components (Table 1). In addition, there are temporal bones available from different ages from embryonic to very old age.

The use of celloidin-embedded sections for IHC has yielded important information regarding the expression of proteins relevant to inner ear structure or homeostasis. Using the preparative methods for IHC described previously (O'Malley et al. 2009a, b) adopted to our laboratory protocol, we have been able to detect Tom20 (translocase of the outer mitochondrial membrane-20) (Balaker et al. 2013), the glutamate transporter (GLAST) (Ahmed et al. 2013), the mu-opioid receptor (Nguyen et al. 2014) and recently neuroglobin (Vorasubin et al. 2016) in celloidin-embedded sections of the human cochlea. The protocol for IF in celloidin-embedded tissue sections described in this review manuscript allows for colocalization of several proteins in a regular fluorescent microscope or confocal microscope (Fig. 5a, b).

##### *Disadvantages*

Decalcification and celloidin embedding of a temporal bone take 1 year. The sectioning of the specimens requires a sliding microtome that uses large-size blades that need to be sharpened frequently. For celloidin-embedded specimens, the orientation of cutting is crucial and histological and IHC staining requires special training. Celloidin, a sulfated and nitrated cellulose, is expensive and requires long infiltration times and is technically much more difficult to work with than paraffin wax or microdissection. Some histochemical staining that requires fresh-frozen fixed or unfixed tissue is not feasible because of dehydration and celloidin embedding. The use and storage of celloidin require experienced personnel, given that it is explosive when not properly handled and stored. Celloidin embedding is not ideal if there is a time limit for production of sections, or if there is not experienced personnel. It is noteworthy that we could not detect nidogen and aquaporins 1, 4, and 6 in celloidin-embedded specimens. However, we have successfully detected these proteins by IF using cryostat sections from microdissected auditory and vestibular endorgans obtained postmortem (Ishiyama et al. 2009; Lopez et al. 2007). These results suggest that prolonged decalcification, celloidin embedding and removal may affect the conformation of the antigen.

Celloidin needs to be removed completely to allow antigen exposure and antibody binding when using either indirect IHC methods (HRP + DAB) or IF. Prolonged decalcification and the type of decalcifying agent may cause loss of antigens. Table 1 lists several antigens identified in celloidin-embedded sections (this manuscript and previous reports by other researchers). Lack of detection by IHC of a given antigen in celloidin-embedded sections should be confirmed using frozen or paraffin sections.

## Alternative human inner ear tissue sources and new imaging methodologies

Human inner ear tissue (cochlea and vestibular endorgans) obtained from ablative surgery has been useful to investigate the expression of several proteins by IHC, mRNA (Ishiyama et al. 2010; Calzada et al. 2012b; Liu et al. 2015, 2016), and ultrastructural organization of the auditory and vestibular sensory epithelium (Ishiyama et al. 2007; McCall et al. 2009; Liu et al. 2015; Taylor et al. 2015). Studies of Cx distribution in the human cochlea: IF and confocal microscopy analysis of Cx proteins in the human cochlea have shown that Cx26 and Cx30 proteins are co-expressed (Liu et al. 2009). Using super-resolution structured illumination fluorescent microscopy (SR-SIM) in fresh human cochlea obtained from surgery, Liu et al. (2016) found that Cx26 and Cx30 are expressed in the lateral wall in separate plaques. As described by Liu et al. (2016), SR-SIM provides structural information below the diffraction limit by superimposing various grid orientations of excitation light on the specimen to generate raw fluorescence images that are reconstructed into high-resolution derivatives. The volume resolution of three-dimensional SIM is approximately eightfold higher than that of a conventional microscopy (Liu et al. 2016; Schermelleh et al. 2008). Recently, scanning thin-sheet laser imaging microscopy (STSLIM) was used in decellularized human inner ear to investigate temporal bone histopathology (Shane et al. 2014) and the organization of the ECM in the cochlea (Santi et al. 2016). We summarize results from these studies below.

### *Immunohistochemistry, scanning thin-sheet laser imaging microscopy (STSLIM) and scanning electron microscopy in decellularized human cochlea*

The application of recent imaging methodologies to the study of the anatomy of human temporal bones has revealed the organization of the ECM and the presence of novel structures. Santi and Johnson (2013) reported on the ECM of the cochlea and vestibular system after decellularization in mouse rat and human at the light microscopic level. To visualize the ECM of the cochlea, sodium dodecyl sulfate (SDS) was used to lyse and remove all cells in fresh, unfixed cochleas. Then, the cochleas were immersed in SDS for 1 week at 4 °C and one more week room temperature. Using a microtome/microscope called STSLIM, Santi and Johnson (2013) examined complete serial sections (approximately 300) of the cochlea. This methodology revealed a new structure on the apical surface of the basilar membrane. Liu et al. (2015) showed that this structure was immunoreactive for laminin and type IV collagen supporting the role of this structure as a component of the ECM. Recently, Santi et al. (2016) examined the anatomy

of the mouse and human cochlea ECM following decellularization using scanning electron microscopy.

### *Further IHC studies in the human temporal bone (celloidin-embedded sections)*

Studies on the identification of several proteins in the human inner ear by IHC and molecular biological techniques are continually expanding. Aggrecan (extracellular component of cartilage), S100 and connective tissue growth factor were detected in the human temporal bones from individuals diagnosed with DFNA9 (McCall et al. 2011). Changes in neurofilaments and myelin protein zero antibodies were detected in the cochlea of a patient with hearing loss caused by the p.L114P COCH mutation (Burgess et al. 2016). Recent studies that apply IHC in human inner ear celloidin-embedded sections have shown the presence of specific markers for macrophages/microglia: CD163<sup>+</sup>, Iba1<sup>+</sup> and CD68<sup>+</sup> (O'Malley et al. 2015). Nadol et al. (2014) identified B (CD20) and T cells (CD3) as well as macrophages (CD68) in temporal bones from individuals that received cochlea implants. Jung et al. (2016) identified CD45 in celloidin sections of an individual diagnosed with recent onset of Cogan's syndrome. Cochlin-IR was detected in the middle ear of normal and DFNA-9 affected human middle ear (Robertson et al. 2014).

## Conclusions and future directions

For all methods described, a longer postmortem time of collection is associated with poor morphology. IHC and confocal studies with triple localization can be made in the three types of tissue sections. Formalin-fixed cryostat sections obtained from microdissected endorgans can be used for IHC and non-radioactive in situ hybridization. Microdissected auditory and vestibular endorgans can be used for morphological, quantitative stereology, IHC and IF studies.

Paraffin-embedded tissue sections can be used for IHC, but there is some loss of antigenicity due to heat and xylene used to embed and remove the paraffin. Some of the structures such as Reissner's membrane may be lost in processing. Formalin-fixed celloidin-embedded human temporal bone sections have been collected and archived for decades and represent a superb source of specimens to study inner ear diseases. Celloidin-embedded tissue sections can be treated with antigen retrieval protocols to be successfully used for IHC. By quenching of auto-fluorescence of celloidin-embedded sections, we have successfully developed a protocol for colocalization using double fluorescence staining ("Appendix" section). The methods of temporal bone processing are not exclusive; for bilateral disease processes, one temporal bone can be processed in

the traditional manner (formalin-fixed celloidin-embedded) and the other can be processed using the microdissection technique. Celloidin-embedded specimens are the preferred methodology to identify new disease entities without previous histopathology (e.g., new hereditary hearing loss syndromes). Frozen or paraffin sections can be used as a pre-screening test for IHC, before celloidin tissue sections are used for this purpose.

In the last decade, an improvement in methodologies specifically designed to prepare human and animal inner ear tissue has helped to show the similarities and differences in the expression of several key proteins expressed in the inner ear. There are still ways to improve temporal bone processing for cellular and molecular biological investigations. For example, there is the need to test contemporary antigen retrieval methods (Shi et al. 2011) using buffers with different pH and periods of microwave heating (Gu et al. 2016). Post-processing methods like CLARITY (Poguzhelskaya et al. 2014) to visualize inner ear tissue in situ. A combination of fast temporal bone harvesting, processing and the use of higher quality of molecular biological reagents (antibodies and mRNA probes) will further contribute to the understanding of the human inner ear cellular composition, and how the inner ear of animal models can help to the design of new therapies for the treatment of disabling inner ear disorders.

**Acknowledgments** This work was supported in part by the National Institutes of Health Grant U24 DC011962-05 (FHL).

**Authors' contributions** IAL, SH, KH, DA and GI were involved in experimental work. IAL, GI, FHL and AI were involved in article preparation. All authors have approved submission of this article.

**Compliance with ethical standards**

**Conflict of interest** None.

## Appendix

### Specimens

The Institutional Review Board (IRB) of UCLA approved this study (IRB #14-001753). Appropriate informed consent for inclusion in the study was obtained from each temporal bone donor. The temporal bone donors used in this study were part of a National Institute of Health funded Human Temporal Bone Consortium for Research Resource Enhancement. Auditory and vestibular endorgans were microdissected from postmortem temporal bones from seven subjects with a documented history of normal auditory and vestibular function. The vestibular endorgans and

**Table 2** Specimens used for IHC (HRP-DAB) and IF

Type of tissue	Age	Gender	PMT (h)	Figures
M	83	Male	6	1c and 3d, e
M	84	Male	9	1d and 3a, b
M	86	Male	8	1e–g and 3c
M	86	Female	7	1h, k and 3h
M	87	Female	9	1a, b, i
M	90	Female	10	1 and 2c, 3f, g
M	95	Female	8	1j, l, l' and 2a, b
A	32	Male	6	4a, a'''
A	47	Male	4	4a', a''
A	48	Male	7	4b, b'
A	63	Female	5	4b''
A	64	Male	7	4e
A	67	Male	9	4c
A	70	Male	11	4d
A	75	Male	8	5a, b

*M* microdissected, auditory and vestibular endorgans were microdissected from the right and left temporal bone and used for frozen or whole-mount IF staining. Normal aging. *A* archival celloidin-embedded tissue sections, normal hearing and vestibular function, tissue sections from the right or left temporal bone were used. *PMT* postmortem time. Figures: images captured after IHC or IF staining. Staining of different antibodies was replicated in some cases (cryostat, paraffin, celloidin sections)

cochlea were microdissected from one temporal bone from each donor. Celloidin-embedded sections were selected from several temporal bones of our temporal bone bank collection. Table 2 shows the source of the specimens used.

### Microdissection of auditory and vestibular endorgans

At autopsy, the whole brain, including the brainstem and blood vessels, was removed from the cranial cavity. The 8th cranial nerve and vascular bundle were sectioned outside the internal auditory canal. The temporal bone was then removed as described by Schuknecht (1968) using a bone plug cutter. The bones were then immediately immersed for 16 h in ice-cold 10 % buffered formalin. Thereafter, the fixative was removed by washing with phosphate buffer (0.1 M, pH 7.2) PB (20 min × 3). Before the auditory and vestibular endorgan microdissection, the connective and muscle tissue was removed. The tympanic membrane and ossicles were then removed, and the temporal bones are immersed in 10 % EDTA (pH 7.4) for 3 days. Temporal bones immersed in EDTA were placed under a dissecting microscope (Nikon SMZ1500), and using forceps, the bone

that surrounds the membranous labyrinth was carefully removed (Lopez et al. 2005a, 2007; Ishiyama et al. 2009). The oval window was identified, and surrounding bone was carefully removed until the utricle was visualized and removed; then, the horizontal and superior crista ampullaris were identified and removed. Thereafter, the saccule and posterior canal were also removed. The bone that surrounds the cochlea was further removed, and the remaining bone that contains the membranous portion of the cochlea was kept in 10 % EDTA for 1 week; then, the bone was carefully removed and the whole cochlea was detached from the bone. The microdissected auditory and vestibular endorgans were placed in 10 % EDTA for one more day, and cryostat sections were obtained.

### Cryostat sections

The whole microdissected cochlea or vestibular endorgan was immersed in 30 % sucrose in PBS for 7 days for cryoprotection. The endorgans were removed from the sucrose solution and immersed in Tissue Tek<sup>®</sup> compound (VWR). Before sectioning, the dissected vestibular endorgans and cochlea were placed on Teflon embedding molds (Polysciences Inc.) and properly oriented under the dissecting microscope to obtain longitudinal mid-modiolar sections of cochlea, and cross sections of the macula utricle or saccule and of the cristae ampullares. Endorgans were placed under vacuum for 4–6 h to allow infiltration of Tissue Tek. Twenty-micron-thick serial sections were obtained using a Microm-H cryostat (Microm-HN505E). Three consecutive sections were placed in each slide. By doing this step, up to six different antibodies can be simultaneously screened (one different monoclonal and one polyclonal antibody per tissue section) per slide. The cryostat sections were mounted on Superfrost Plus glass slides (Fisher Scientific, Pittsburgh, PA, USA) and stored at  $-80^{\circ}\text{C}$  until they were used. Cryostat sections properly stored can be used for IHC several years after being sectioned. Before that IHC sections were thawed and allowed to dry for 30 min. Next, with the aid of a pen that contains hydrophobic solution (ImmEdge pen, Vector) a line around each tissue section was made to prevent the mixture of the different solutions.

### Immunofluorescence

After thawing at room temperature for 10 min, tissue sections were incubated at room temperature for 60 min with a blocking solution containing 1 % bovine serum albumin (BSA) fraction V (Sigma, St. Louis, MO, USA) and 0.5 % Triton X-100 (Sigma) in PBS. At the end of the incubation, the blocking solution was removed and the primary

polyclonal or monoclonal antibody against the specific protein was applied (Table 3). Primary antibodies were incubated overnight at  $4^{\circ}\text{C}$  in a humidity chamber. The secondary antibodies against rabbit or mouse labeled with Alexa 488 or 594 (1:1000, Molecular Probes, Carlsbad, CA, USA) were applied and incubated for 2 h at room temperature in the dark. At the end of the incubation, sections were washed with PBS ( $3 \times 10$  min) and covered with Vectashield mounting media containing DAPI (Vector Labs, Burlingame, CA, USA) to visualize all cell nuclei.

### Antibodies

The characteristics and specificity of the antibodies used in this study have been described in detail (Duong et al. 2011; Ishiyama et al. 2009, 2010; Lopez et al. 2005a, 2007, 2009; Calzada et al. 2012a, b; Balaker et al. 2013; Ahmed et al. 2013; Nguyen et al. 2014; Vorasubin et al. 2016) (Table 3).

### Controls

As positive controls, human kidney and brain (cerebral and cerebellar cortex) cryostat sections from the same subjects were used. These sections were subjected to the same protocol as the IF protocol of vestibular endorgans and cochlea cryostat sections. As negative controls, the primary antibody was omitted and the immunoreaction was performed as described above. In all cases, no immunoreaction was detected.

### Quality of frozen sections obtained from microdissected endorgans

It is well known that longer post-mortem times are associated with poorer morphology as demonstrated on hematoxylin and eosin staining (Ishiyama et al. 2009). The immunoreactive pattern in the tissue from the temporal bones used in this, and previous studies give similar results.

### IF staining in whole auditory and vestibular endorgans

The microdissected whole cristae, macula utricle, or cochlea was immersed in 30 % sucrose in PBS (0.1 M, pH 7.4) for 1 week. Individual endorgans were subjected to a freezing step that was accomplished after removing most of the sucrose solution from the container, leaving only enough solution to cover the tissue. For the freezing step, auditory or vestibular endorgans were placed in a plastic vial and immersed in liquid nitrogen and immediately thereafter removed, and the endorgans were left to thaw for 5 min and the sucrose solution replaced by PBS before IF staining (Lopez et al. 2005a).

**Table 3** Antibodies used in the present study

Antibody/source	Dilution/antibody type	SR	Negative control	Positive control
Acetylated tubulin/Sigma	1: 1000/mouse monoclonal	Human, mouse, rat	No antibody in the IHC	Mouse cochlea
Aquaporin-4/Santa Cruz	1:1000/rabbit polyclonal	Human, mouse, rat	No antibody in the IF	Mouse and rat cochlea and kidney
Collagen IV $\alpha$ /Chemicon	1:1000/mouse monoclonal	Human, rat, mouse	No antibody in the IHC	Mouse cochlea
Cochlin/Santa Cruz	1:500/goat polyclonal	Human, mouse	No antibody	Mouse cochlea
Connexin 26/Thermo Scientific	1:200/rabbit polyclonal	Human	No antibody on IF	Mouse cochlea
Connexin 30/Millipore	1:500/rabbit polyclonal	Human, mouse	No antibody on IF	Mouse cochlea
GFAP/Sigma	1:250/mouse monoclonal	Human	No antibody on IF	Human brain cortex
Kir 4.1/Alomone	1:500/rabbit polyclonal	Human, mouse	No antibody on IF	Mouse cochlea
Myosin VIIa/Abcam	1:100/rabbit polyclonal	Human, mouse	No antibody on IF	Mouse cochlea
Laminin- $\beta$ 2/Upstate	1:250/rat polyclonal	Human, mouse, rat	No antibody	Mouse cochlea
Mitochondria/Chemicon	1:500/rabbit polyclonal	Human	No antibody on IF	Human brain cortex
Na <sup>+</sup> K <sup>+</sup> -ATPase $\alpha$ 2 subunit/ Hybridoma bank	1:1000/rabbit polyclonal	Mouse, human	No antibody in the IHC	Mouse cerebellar cortex
Prestin/Santa Cruz	1:250/rabbit polyclonal	Human, mouse, rat	Antibody absorption with peptide	Mouse cochlea
Pan neurofilaments/Zymed	1:1000/mouse monoclonal	Human, mouse, rat	No antibody in the IHC or IF	Mouse cerebellar cortex
$\alpha$ -Smooth muscle actin/ Sigma	1:1000/mouse monoclonal	Human, rat	No antibody on IF	Mouse cerebellar cortex
SOD-2/Abcam	1:250/rabbit polyclonal	Human	No antibody on IF	Mouse cerebellar cortex
WARP/Sigma	1:100/rabbit polyclonal	Human	No antibody IHC or IF	Human, mouse cerebellar cortex

Dilution: all in PBS

SR species reactivity, IHC immunohistochemistry, IF immunofluorescence

### Immunofluorescence (IF)

The endorgans were placed in a rotary shaker and incubated for 3 h in a blocking solution containing 2 % BSA fraction V (Sigma, SLM), 0.1 % TritonX-100 (Sigma, SLM) diluted in PBS at 4–6 °C. Subsequently, the blocking solution is removed and the whole organs are incubated for 48 h with the primary antibodies (Table 3), placing the vials in the rotatory shaker in a cold room. At the end of the incubation, the secondary antibodies against rabbit labeled with Alexa 594 were diluted 1:1000 in PBS (Molecular Probes, Eugene, OR, USA) or the secondary antibodies against mouse labeled with Alexa 488 (1:1000 in PBS, Molecular Probes) were applied to the tissue sections and were incubated for 1 h at room temperature in the dark. At the end of the incubation, the whole endorgans or sections were washed with PBS (20 min  $\times$  5) and mounted flat on glass slides with Vectashield solution containing DAPI (Vector Labs, Burlingame, CA, USA) and immediately coverslipped. The coverslip was attached to the glass slide using nail polish around the glass slide.

### Phalloidin staining in whole endorgans

Following microdissection and permeabilization steps, vestibular endorgans were incubated in a blocking solution that contained 1 % BSA (Sigma, Fraction V) for 1 h and then phalloidin Oregon Green (20 units–10  $\mu$ L, Molecular Probes) for 15 min. Following incubation at room temperature, the tissue was washed with PBS and mounted on glass slides as described above for IF.

### IHC in paraffin-embedded tissue sections

After microdissection from the temporal bone, the cochlea and the vestibular endorgans were placed overnight in 10 % EDTA (in PB, pH 7.4) on a rotary shaker. The specimens were then washed twice in PB for 15 min. Specimens underwent dehydration by serial immersion for 5 min each in an increasing concentration of ethanol as follows: 35, 50, 70, 95 then 100 %. The specimens were then transferred to a 1:1 mixture of 100 % ethanol and 100 % xylene for 5 min and placed in the oven at 65 °C for 5 min. Using a



wood stick, the endorgans were then transferred to melted paraffin and placed in the oven for 5 min at 60 °C. Specimens were placed in individual Teflon-coated silicon molds (Polysciences) filled with melted paraffin and properly oriented to obtain mid-modiolar sections of the cochlea, and cross sections of the cristae ampullares, maculae utricle and saccule. Ten-micron-thick paraffin sections were obtained using a paraffin microtome (Leica, RM216S). The sections were then immediately mounted onto Superfrost Plus slides (Fisher Scientific, Pittsburgh, PA, USA). The slides were dried on a slide warming plate for 30 min and stored at room temperature until use for IHC.

### Deparaffinization

The slides with the tissue sections were placed in the oven at 65 °C for 10 min to remove paraffin. Slides were placed in a slide tray and immersed in 100 % xylene (5 × 3 min). Rehydration was performed by immersion with graded dilutions of ethanol (Fisher Scientific) for 5 min in each dilution as follows: 100 % three times, 70 % then 50 %. The slides were then placed in double distilled water and PBS for 10 min each.

### Indirect IHC

Endogenous peroxidase inactivation in deparaffinized sections was performed by incubation for 10 min with 3 % hydrogen peroxide (diluted in 100 % in methanol). Slides were then washed with PBS for 10 min and then transferred to a Teflon slide carrier filled with antigen retrieval solution (Vector Antigen Unmasking Solution, Vector Labs, Burlingame, CA, USA) diluted 1:200 with double distilled water and heated in the microwave for a total of 5 min. The slides were cooled and transferred to a PBS wash for 10 min. Sections were incubated for 30 min with blocking solution containing 3 % normal rabbit or horse serum and 0.5 % Triton X-100 (Sigma) in PBS. Incubation with the respective primary antibody (Table 3) was performed for 48 h at 4 °C in a humid chamber. The sections were washed with PBS (3 × 5 min). Next, sections were incubated for 1 h with biotinylated secondary antibody, goat anti-rabbit polyclonal IgG (1:1000, Vector Labs, Burlingame, CA, USA). Afterward, sections were washed PBS (10 min × 3). Next, 1-h incubation was performed with Vectastain Elite ABC reagent (Vector Labs) followed by PBS washes (10 min × 3). Immunoperoxidase staining was performed using ImmPACT<sup>®</sup> diaminobenzidine (DAB) solution (Vector Labs). The immunoreaction was stopped with PBS washes (10 min × 3). Slides were mounted with VectaMount AQ aqueous mounting media (Vector Labs) and glass cover slips.

### IHC in celloidin-embedded sections

The methodology to mount celloidin-embedded sections, celloidin removal and antigen retrieval steps has been described in detail (O'Malley et al. 2009a, b; Shi et al. 1998) and used as described by our laboratory for the processing of human archival temporal bones (Ahmed et al. 2013; Balaker et al. 2013; Nguyen et al. 2014; Vorasubin et al. 2016). In brief, sections were removed from the archival jar and immediately floated 80 % ethanol and mounted on subbed glass slides (Superfrost Plus glass slides, Thermo Scientific). Bibulous paper (soaked with 10 % formalin) was placed over the section. A small roller was used to flatten the sections. A block of wood was placed over each slide. Sections were allowed to dry for 1 day, and the weight and the bibulous paper were removed.

### Celloidin removal

A stock solution of sodium ethoxide was diluted with ethanol 1:3 (50 mL of this mixture is used per section). Celloidin sections previously mounted on Superfrost plus glass slides (O'Malley et al. 2009a) were placed in a glass Petri dish and immersed in the diluted solution for 30 min. Thereafter, sections were sequentially immersed in: 100 % acetone (30 min), 100 % methanol, 70, 50 % and distilled water (5 min each) and then immersed in hydrogen peroxide 5 % in methanol (10 min). Slides were then washed with distilled water before the antigen retrieval step.

### Antigen retrieval

Glass slides with the tissue sections attached were placed horizontally in a glass Petri dish that contains antigen retrieval solution (Vector Antigen Unmasking Solution, Vector Labs, Burlingame, CA, USA), prepared at the time of use, diluted 1:200 with distilled water. Sections were heated in the microwave oven using intermittent heating methods of two 2-min cycles with and interval of 2 min between the heating cycles. The Petri dish containing the slides was removed from the microwave oven and allowed to cool for 15 min (room temperature) and washed with PBS for 10 min prior to IHC.

### Indirect IHC

After antigen retrieval treatment, the celloidin sections were immunoreacted using the same protocol described above for paraffin-embedded tissue sections. Primary antibodies were incubated for 48 h at room temperature (Table 3). At the end of the IHC, the sections are covered

with a water-soluble mounting media (Aqua-polymount, Polysciences) and let them dry for 1 day and imaged.

## Indirect immunofluorescence in celloidin-embedded sections

### Quenching of auto-fluorescence for immunofluorescence staining

After the antigen retrieval step, the sections were placed in a glass Petri dish containing iced cold PBS and placed in a UV chamber for 8 h. Temperature was checked constantly to avoid heating, and cold PBS was replaced every 30 min. This quenching step was mandatory to remove auto-fluorescence intrinsic to the human temporal bone sections. The presence of auto-fluorescence was checked before and after UV exposure. Sections were processed for IF once the auto-fluorescence signal in the tissue sections has disappeared.

### Immunofluorescence

After auto-fluorescence was completely removed, the celloidin sections were immunostained using the same protocol described above for IF in formalin-fixed cryostat sections of the inner ear. The incubation step with hydrogen peroxide was omitted in tissue sections used for IF. Primary antibodies against prestin and acetylated tubulin (Table 3) were incubated for 48 h at room temperature.

### Microscopic observation and documentation

Immunoreacted tissue sections were viewed and captured using an Olympus BX51 fluorescent microscope (Olympus America Inc., NY, USA) equipped with an Olympus DP70 digital camera. All images were captured using the same camera settings. Images were acquired using MicroSuite™ Five software (Olympus America Inc.). All images were prepared using the Adobe Photoshop™ software program run in a Dell Precision 380 computer. Confocal microscope images were acquired with a Carl Zeiss Laser scanning microscope model LSM 510 Meta Zeiss (Jena, Germany).

## References

- Aarnisalo AA, Green KM, O'Malley J, Makary C, Adams J, Merchant SN, Evans JE (2010) A method of MS differential proteomic analysis of archival formalin-fixed celloidin-embedded human inner ear tissue. *Hear Res* 270(1–2):15–20
- Ahmed S, Vorasubin N, Lopez IA, Hosokawa S, Ishiyama G, Ishiyama A (2013) The expression of glutamate aspartate transporter (GLAST) within the human cochlea and its distribution in various patient populations. *Brain Res* 5:134–142
- Anniko M, Arnold W, Thornell LE (1989a) Localization of the integral membrane glycoprotein synaptophysin and the surface glycoprotein Egp-34 in the embryonic and adult human inner ear ORL. *J Otorhinolaryngol Relat Spec* 51(4):221–228
- Anniko M, Thornell LE, Ramaekers FC, Stigbrans T (1989b) Cytokeratin diversity in epithelia of the human inner ear. *Acta Otolaryngol* 108(5–6):385–396
- Arnold W (1988) Immunohistochemical investigation of the human inner ear. Limitations and prospects. *Acta Otolaryngol* 105(5–6):392–397
- Balaker AE, Ishiyama P, Lopez IA, Ishiyama G, Ishiyama A (2013) Immunocytochemical localization of the translocase of the outer mitochondrial membrane (Tom20) in the human cochlea. *Anat Rec* 296(2):326–332
- Battifora H, Kopinski M (1986) The influence of protease digestion and duration of fixation on the immunostaining of keratins. A comparison of formalin and ethanol fixation. *J Histochem Cytochem* 34:1095–1100
- Bauwens LJ, Veldman JE, Huizing EH (1990) Progress in temporal bone histopathology. III. An improved technique for immunohistochemical investigation of the adult inner ear. *Acta Otolaryngol Suppl* 470:34–39
- Burgess BJ, O'Malley JT, Kamakura T, Kristiansen K, Robertson NG, Morton CC, Nadol JB Jr (2016) Histopathology of the human inner ear in the p. L114P COCH mutation (DFNA9). *Audiol Neurootol* 21(2):88–97
- Calzada A, Lopez IA, Ishiyama A, Beltran-Parrazal L, Ishiyama G (2012a) Cochlin expression in vestibular endorgans obtained from patients with Meniere's disease. *Cell Tissue Res* 350(2):373–384
- Calzada A, Balaker A, Ishiyama G, Lopez IA, Ishiyama A (2012b) Temporal bone histopathology and immunoglobulin depositions in Sjogren's syndrome. *Otol Neurotol* 33(2):258–266
- Chole RA (2010) Labs in crisis: protecting the science-and-art-of otopathology. *Otol Neurotol* 31(4):554–556
- Cunningham CD III, Schulte BA, Bianchi LM, Weber PC, Schmiedt BN (2001) Microwave decalcification of human temporal bones. *Laryngoscope* 111(2):278–282
- Doherty JK, Linthicum FH (2004) Spiral ligament and stria vascularis changes in cochlear otosclerosis: effect on hearing level. *Otol Neurotol* 25(4):457–464
- Duong T, Lopez IA, Ishiyama G (2011) Immunocytochemical distribution of WARP (von Willebrand A domain-related protein) in the inner ear. *Brain Res* 1367:50–61
- Fish JH III, Scholtz AW, Hussl B, Kammen-Jolly K, Ichiki H, Kreczy A, Schrott-Fischer A (2000) Immunohistochemical and morphological studies in the human fetal cochlea: a comparative view on methods. *Tissue Cell* 33(2):189–199
- Ganbo T, Sando I, Balaban CD, Suzuki C, Sudo M (1997) Immunohistochemistry of lymphocytes and macrophages in human celloidin-embedded temporal bone sections with acute otitis media. *Ann Otol Rhinol Laryngol* 106(8):662–668
- Ganbo T, Sando I, Balaban CD, Suzuki C, Kitagawa M (1999) Inflammatory response to chronic otitis media in DiGeorge syndrome: a case study using immunohistochemistry on archival temporal bone sections. *Am Otol Rhinol Laryngol* 108(8):756–761
- Gardella D, Hatton WJ, Rind HB, Rosen GD, von Bartheld CS (2003) Differential tissue shrinkage and compression in the z-axis: implications for optical dissector counting in vibratome-, plastic- and cryo-sections. *J Neurosci Methods* 124(1):45–59
- Gopen Q, Lopez I, Ishiyama G, Baloh RW, Ishiyama A (2003) Unbiased stereologic type I and type II hair cell counts in human utricular macula. *Laryngoscope* 113(7):1132–1138

- Goran B (1968) Cellular pattern and nerve supply of the human organ of Corti. *Acta Otolaryngol Suppl* 236:1–35
- Gu L, Cong J, Zhang J, Tian YY, Zhai XY (2016) A microwave antigen retrieval method using two heating steps for enhanced immunostaining on aldehyde-fixed paraffin-embedded tissue sections. *Histochem Cell Biol* 145:675–680
- Guild SR (1921) A graphic reconstruction method for the study of the organ of Corti. *Anat Rec* 22:141–157
- Gulya AJ (2007) Gulya and Schuknecht's anatomy of the temporal bone with surgical implications, 3rd edn. Informa Healthcare, New York
- Heaney DL, Schulte BA, Niedzielski AS (2002) Dystroglycan expression in the developing and senescent gerbil cochlea. *Hear Res* 174(1–2):9–18
- Ishiyama A, López I, Wackym P (1994) Choline acetyltransferase immunoreactivity in the human vestibular end-organs. *Cell Biol Int* 18(10):979–984
- Ishiyama A, Lopez I, Ishiyama G, Tang Y (2004) Unbiased quantification of the microdissected human Scarpa's ganglion neurons. *Laryngoscope* 114(8):1496–1499
- Ishiyama A, Mowry SE, Lopez IA, Ishiyama G (2009) Immunohistochemical distribution of basement membrane proteins in the human inner ear. *Hear Res* 254(1–2):1–14
- Ishiyama G, Lopez IA, Beltran-Parrasal L, Ishiyama A (2010) Immunohistochemical localization and mRNA expression of aquaporins in the macula utriculi of patients with Meniere's disease and acoustic neuroma. *Cell Tissue Res* 340(3):407–419
- Jokay I, Soos G, Repassy G, Dezso B (1998) Apoptosis in the human inner ear. Detection by in situ end-labeling of fragmented DNA and correlation with other markers. *Hear Res* 117:131–139
- Jung DH, Nadol JB Jr, Folkert RD, Merola JF (2016) Histopathology of the inner ear in a case with recent onset of Cogan's syndrome: evidence for vasculitis. *Ann Otol Rhinol Laryngol* 125(1):20–24
- Kammen-Jolly K, Ichiki H, Scholtz AW, Gsenger M, Kreczy A, Schrott-Fisher A (2001) Connexin 26 in human fetal development of the inner ear. *Hear Res* 160:15–21
- Keithley EM, Tian Q, Robins-Browne R (1994) Fibronectin-like immunoreactivity of the basilar membrane of celloidin-embedded human temporal bone sections. *Acta Otolaryngol* 114(6):613–619
- Keithley EM, Horowitz S, Ruckenstein MJ (1995) Na<sup>+</sup>, K<sup>+</sup>-ATPase in the cochlear lateral wall of human temporal bones with endolymphatic hydrops. *Ann Otol Rhinol* 104(11):858–863
- Keithley EM, Truong T, Chandronait B, Billings PB (2000) Immunohistochemistry and microwave decalcification of human temporal bones. *Hear Res* 148(1–2):192–196
- Keithley EM, Harris B, Desai K, Linthicum F, Fishel-Ghodsian N (2001) Mitochondrial cytochrome oxidase immunolabeling in aged human temporal bones. *Hear Res* 157(1–2):93–99
- Khalifa SA, Friberg U, Illing RB, Rask-Andersen H (2003) Synaptophysin immunohistochemistry in the human cochlea. *Hear Res* 185(1–2):35–42
- Khetarpal U (2000) DFNA9 is a progressive audiovestibular dysfunction with a microfibrillar deposit in the inner ear. *Laryngoscope* 110:1379–1384
- Kong WJ, Hussl B, Thumfart WF, Schrott-Fisher A (1998) Ultrastructural localization of GABA-like immunoreactivity in the human utricular macula. *Hear Res* 119(1–2):104–112
- Liu W, Bostrom M, Kinnefors A, Rask-Andersen H (2009) Unique expression of connexins in the human cochlea. *Hear Res* 250(1–2):55–62
- Liu W, Atturo F, Aldaya R, Santi P, Cureoglu S, Obwegeser S, Glueckert R, Pfäller K, Schrott-Fisher A, Rask-Andersen H (2015) Macromolecular organization and fine structure of the human basilar membrane—RELEVANCE for cochlear implantation. *Cell Tissue Res* 360:245–262
- Liu W, Edin F, Blom H, Magnusson P, Schrott-Fischer A, Glueckert R, Santi PA, Li H, Laurell G, Rask-Andersen H (2016) Super-resolution structured illumination fluorescence microscopy of the lateral wall of the cochlea: the connexin 26/30 proteins are separately expressed in man. *Cell Tissue Res*. doi:10.1007/s00441-016-2359-2370
- Lopez I, Ishiyama G, Tang Y, Frank M, Baloh RW, Ishiyama A (2005a) Estimation of the number of nerve fiber in the human vestibular endorgans using unbiased stereology and immunohistochemistry. *J Neurosci Methods* 145(1–2):37–46
- Lopez I, Ishiyama G, Tang Y, Tokita J, Baloh RW, Ishiyama A (2005b) Regional estimates of hair cells and supporting cells in the human crista ampullaris. *J Neurosci Res* 82(3):421–431
- Lopez IA, Ishiyama G, Lee M, Baloh RW, Ishiyama A (2007) Immunohistochemical localization of aquaporins in the human inner ear. *Cell Tissue Res* 328(3):453–460
- Maekawa C, Kitahara T, Kizawa K, Okazaki S, Kamakura T, Horii A, Imai T, Doi K, Inohara H, Kiyama H (2010) Expression and translocation of aquaporin-2 in the endolymphatic sac in patients with Meniere's disease. *J Neuroendocrinol* 22:1157–1164
- Markaryan A, Nelson EG, Tretiakova M, Hinojosa R (2008a) Technical report: laser microdissection of cochlear structures from celloidin embedded human temporal bone tissues and detection of the mitochondrial DNA common deletion using real time PCR. *Hear Res* 244(1–2):1–6
- Markaryan A, Nelson EG, Tretiakova M, Hinojosa R (2008b) Technical report: immunofluorescence and TUNEL staining of celloidin embedded human temporal bone tissues. *Hear Res* 241(1–2):1–6
- Markaryan A, Nelson EG, Hinojosa R (2008c) Detection of mitochondrial DNA deletions in the cochlea and its structural elements from archival temporal bone tissue. *Mutat Res* 640(1–2):38–45
- Markaryan A, Nelson EG, Hinojosa R (2009) Quantification of the mitochondrial DNA common deletion in presbycusis. *Laryngoscope* 119(6):1184–1189
- Markaryan A, Nelson EG, Helseth LD, Hinojosa R (2010a) Proteomic analysis of formalin-fixed celloidin-embedded whole cochlear and laser microdissected spiral ganglion tissues. *Acta Otolaryngol* 130(9):984–989
- Markaryan A, Nelson EG, Hinojosa R (2010b) Major arc mitochondrial deletions in cytochrome c oxidase-deficient human cochlear spiral ganglion cells. *Acta Otolaryngol* 130(7):780–787
- Markaryan A, Nelson EG, Kohut RI, Hinojosa R (2011) Dual immunofluorescence staining of proteoglycans in human temporal bones. *Laryngoscope* 121:1525–1531
- McCall A, Ishiyama G, Lopez IA, Sunita B, Ishiyama A (2009) Histopathological and ultrastructural analysis of vestibular endorgans obtained from patients with Meniere's disease. *BMC Ear Nose Throat Disord* 9:4
- McCall AM, Linthicum FH Jr, O'Malley JT, Adams JC, Merchant SN, Bassim MK, Gellibolian R, Fayad JN (2011) Extralabyrinthine manifestations of DFNA9. *J Assoc Res Otolaryngol* 12:141–149
- Merchant SN (1999) A method for quantitative assessment of vestibular otopathology. *Laryngoscope* 109(10):1560–1569
- Merchant SN (2010) Methods of removal, preparation, and study, chap 1. In: Merchant SN, Nadol JB Jr (eds) Schuknecht's pathology of the ear, 3rd edn. PMPH-USA, Shelton CT, USA, pp 3–51
- Merchant SN, Schuknecht HF, Rauch SD, McKenna MJ, Adams JC, Wudarsky R, Nadol JB Jr (1993) The national temporal bone, hearing, and balance pathology resource registry. *Arch Otolaryngol Head Neck Surg* 119(8):846–853

- Merchant SN, Burges B, O'Malley J, Jones D, Adams JC (2006) Polyester wax: a new embedding medium for the histopathologic study of human temporal bones. *Laryngoscope* 116(2):245–249
- Merchant SN, McKenna MJ, Adams JC, Nadol JB, Fayad J, Gellibolian R, Linthicum FH, Ishiyama A, Lopez I, Ishiyama G, Baloh R, Platt C (2008) Human temporal bone consortium for research resource enhancement. *J Assoc Res Otolaryngol* 9(1):1–4
- Nadol JB, Cho YBM, Burgess BJ, Adams JC (1993) The immunolocalization of synaptophysin in the organ of Corti of the human as shown by immunoelectron microscopy. *Acta Otolaryngol* 113(3):312–317
- Nadol JB Jr, O'Malley JT, Burgess BJ, Galler D (2014) Cellular immunologic responses to cochlear implantation in the human. *Hear Res* 318:11–17
- Nelson EG, Hinojosa R (2014) Analysis of the hyalinization reaction in otosclerosis. *JAMA Otolaryngol Head Neck Surg* 140(6):555–559
- Nguyen KD, Mowlds D, Lopez IA, Hosokawa S, Ishiyama A, Ishiyama G (2014) Mu-opioid receptor (MOR) expression in the human spiral ganglia. *Brain Res* 1590:10–19
- O'Malley JT, Burgess BJ, Jones DD, Adams JC, Merchant SN (2009a) Techniques of celloidin removal from temporal bone sections. *Ann Otol Rhinol Laryngol* 118(8):435–441
- O'Malley JT, Merchant SN, Burgess BJ, Jones DD, Adams JC (2009b) Effects of fixative and embedding medium on morphology and immunostaining of the cochlea. *Audiol Neurotol* 14(2):78–87
- O'Malley JT, Nadol JB Jr, McKenna MJ (2015) Anti CD163+, Iba1+, and CD68+ cells in the adult human inner ear: normal distribution of an unappreciated class of macrophages/microglia and implications for inflammatory otopathology in humans. *Otol Neurotol* 37:99–108
- O'Rourke MB, Padula MP (2016) Analysis of formalin-fixed, paraffin-embedded (FFPE) tissue via proteomic techniques and misconceptions of antigen retrieval. *Biotechniques* 60:229–238
- Pagedar NA, Wang W, Davis RR, Lopez I, Wright CG, Alagramam KN (2006) Gene expression analysis of distinct population of cells isolated from mouse and human inner ear FFPE tissue using laser capture microdissection. *Mol Brain Res* 1091(1):289–299
- Philipp J, Ochs M (2013) Alterations of mouse lung tissue dimensions during processing for morphometry: a comparison of methods. *Am J Physiol Lung Cell Mol Physiol* 306:341–350
- Poguzhelskaya E, Artamonov D, Bolshakova A, Vlasova O (2014) Simplified method to perform CLARITY imaging. *Mol Neurodegener* 9:19
- Popper P, Ishiyama A, Lopez I, Wackym P (2002) Calcitonin gene-related peptide and choline acetyltransferase colocalization in the human vestibular periphery. *Audiol Neurootol* 7(5):298–302
- Rask-Andersen H, Tylstedt S, Kinnefors A, Illing RB (2000) Synapses on human spiral ganglion cells: a transmission electron microscopy and immunohistochemical study. *Hear Res* 141(1–2):1–11
- Richard C, Doherty JK, Fayad JN, Cordero A, Linthicum FH Jr (2015) Identification of target proteins involved in cochlear otosclerosis. *Otol Neurotol* 36(5):923–931
- Robertson NG, Resendes BL, Lin JS, Lee C, Aster JC, Adams JC, Morton CC (2001) Inner ear localization of mRNA and protein products of COCH, mutated in the sensorineural deafness and vestibular disorders, DFNA9. *Hum Mol Genet* 10(22):2493–2500
- Robertson NG, Cremers CWRJ, Huygen PLM, Ikezono T, Krastins B, Kremer H, Kuo SF, Liberman C, Merchant SN, Miller CE, Nadol JB Jr, Sarracino DA, Verhagen WIM, Morton CC (2006) Cochlin immunostaining of inner ear pathologic deposits and proteomic analysis in DFNA9 deafness and vestibular dysfunction. *Hum Mol Genet* 15(7):1071–1085
- Robertson NG, O'Malley JT, Ong CA, Giersch ABS, Shen J, Stankovic KM, Morton CC (2014) Cochlin in normal middle ear and abnormal middle ear deposits in DFNA9 and Coch<sup>G88E/G88E</sup> mice. *J Assoc Res Otolaryngol* 15:961–974
- Rosenhall U (1972) Vestibular macular mapping in man. *Ann Otol* 81(3):339–351
- Rosenhall U, Rubin W (1975) Degenerative changes in the human vestibular sensory epithelia. *Acta Otolaryngol* 79(1–2):67–80
- Santi PA, Johnson SB (2013) Decellularized ear tissues as scaffolds for stem cell differentiation. *J Assoc Res Otolaryngol* 14:3–15
- Santi PA, Aldaya R, Brown R, Johnson S, Stromback T, Cureoglu S, Rask-Andersen H (2016) Scanning electron microscopic examination of the extracellular matrix in the decellularized mouse and human cochlea. *J Assoc Res Otolaryngol*. doi:10.1007/s10162-016-0562-z
- Schermelleh L, Carlton PM, Haase S, Shaoe L, Winoto L, Kner P, Burke B, Cardoso MC, Agards DA, Gustafsson MG, Leonhardt H, Sedat JW (2008) Subdiffraction multicolor imaging of the nuclear periphery with 3D structured illumination microscopy. *Science* 320:1332–1336
- Schrott-Fischer A, Egg G, King WJ, Renard N, Eybalin M (1994) Immunocytochemical detection of choline acetyltransferase in the human organ of Corti. *Hear Res* 78(2):149–157
- Schrott-Fischer A, Kammen-Jolly K, Scholtz AW, Gluckert R (2002a) Patterns of GABA-like immunoreactivity in efferent fibers of the human cochlea. *Hear Res* 174:75–85
- Schrott-Fischer A, Kammen-Jolly K, Scholtz A, Kong WJ, Eybalin M (2002b) Neurotransmission in the human labyrinth. *Adv Otorhinolaryngol* 59:11–17
- Schrott-Fischer A, Kammen-Jolly K, Scholtz A, Rask-Andersen H, Glueckert R, Eybalin M (2007) Efferent neurotransmitters in the human cochlea and vestibule. *Acta Otolaryngol* 127(1):13–19
- Schuknecht HF (1968) Temporal bone removal at autopsy. Preparation and uses. *Arch Otolaryngol* 87:129–137
- Schuknecht HF (1993) Methods of removal, preparation, and study. In: Schuknecht HF (ed) *Pathology of the ear*, 2nd edn. Lea and Febiger, Philadelphia, pp 1–3
- Shane BJ, Cureoglu S, O'Malley JT (2014) Comparison of traditional histology and TSLIM optical sectioning of human temporal bones. *Otol Neurotol* 35(1145):1149
- Shi SR, Key ME, Karla KL (1991) Antigen retrieval in formalin-fixed, paraffin-embedded tissues: an enhancement method for immunohistochemical staining based on microwave oven heating of tissue sections. *J Histochem Cytochem* 39(6):741–748
- Shi SR, Tandon AK, Cote C, Kalra KL (1992a) S-100 protein in human inner ear: use of a novel immunohistochemical technique on routinely processed, celloidin human temporal bone sections. *Laryngoscope* 102(2):734–738
- Shi SR, Cote C, Kalra KL, Taylor CR, Tandon AK (1992b) A technique for retrieving antigens in formalin-fixed routinely acid-decalcified, celloidin-embedded human temporal bone sections for immunohistochemistry. *J Histochem Cytochem* 40(6):787–792
- Shi SR, Tandon AK, Haussmam RR, Kalra KL, Taylor CR (1993) Immunohistochemical study of intermediate filament proteins on routine processed celloidin-embedded human temporal bone sections by using new technique for antigen retrieval. *Acta Otolaryngol* 113(1):48–54
- Shi SR, Cote RJ, Taylor CR (1998) Antigen retrieval immunohistochemistry used for routinely processed celloidin-embedded human temporal bone sections: standardization and development. *Auris Naus Larynx* 25(4):425–443
- Shi SR, Shi Y, Taylor CR (2011) Antigen retrieval immunohistochemistry: review and future prospects in research and diagnosis over two decades. *J Histochem Cytochem* 59(1):13–32
- Swartz DJ, Santi PA (1999) Immunolocalization of tenascin in the chinchilla inner ear. *Hear Res* 130(1–2):108–114

- Takahashi M, Kimura Y, Sawabe M, Kitamura K (2010) Modified paraffin-embedding method for the human cochlea that reveals a fine morphology and excellent immunostaining results. *Acta Otolaryngol* 130(7):788–792
- Tang Y, Nyengaard JR (1997) A stereological method for estimating the total length and size of myelin fibers in human white matter. *J Neurosci Methods* 73:193–200
- Taylor RR, Jagger DJ, Saeed R, Axon P, Donnelly N, Tysome J, Mofatt D, Irving R, Monksfield P, Coulson C, Freeman SR, Lloyd SK, Forge A (2015) Characterizing human vestibular sensory epithelia for experimental studies: new hair bundles on old tissue and implications for therapeutic interventions in ageing. *Neurobiol Aging* 36(6):2068–2084
- Tian Q, Linthicum FH Jr, Keithley EM (1999) Application of labeling techniques to archival temporal bone sections. *Ann Otol Rhinol Laryngol* 108(1):47–53
- Viana LM, O'Malley JT, Burgerss BJ, Jones DD, Oliveira CACP, Santor F, Merchant SN, Liberman LD, Liberman MC (2015) Cochlear neuropathy in human presbycusis: confocal analysis of hidden hearing loss in post-mortem tissue. *Hear Res* 327:78–88
- Vorasubin N, Hosokawa S, Hosokawa K, Ishiyama G, Ishiyama A, Lopez IA (2016) Neuroglobin immunoreactivity in the human inner ear. *Brain Res* 1630:56–63
- Wackym PA, Micevych PE, Wards PH (1990) Immunoelectron microscopy of the human inner ear. *Laryngoscope* 100:447–454
- Wackym P, Chen CT, Ishiyama A, Pettis RM, Lopez I, Hoffman L (1996) Muscarinic acetylcholine receptor subtype mRNAs in the human and rat vestibular periphery. *Cell Biol Int* 20(3):187–192
- Wright C, Meyerhoff WL (1989) Microdissection in human temporal bone morphology. *Ann Otol Rhinol Laryngol Suppl* 143:25–28
- Yamashita H, Bager-Sjoberg D, Wersall J (1991) The presence of laminin in the fetal human inner ear. *Eur Arch Otorhinolaryngol* 248(8):479–482
- Yamashita H, Sekitani T, Bager-Sjoberg D (1992) Expression of carbonic anhydrase isoenzyme-like immunoreactivity in the limbus spiralis of the human fetal cochlea. *Hear Res* 64(1):118–122
- Ying YLM, Balaban CD (2009) Regional distribution of manganese superoxide dismutase 2 (Mn SOD2) expression in rodent and primate spiral ganglion cells. *Hear Res* 253(1–2):116–124
- Zehnder AF, Adams JC, Santi PA, Kristiansen AG, Wacharasindhu C, Mann S, Kalluri R, Gregory MC, Kashtan CE, Merchant SN (2005) Distribution of type IV collagen in the cochlea in Alport syndrome. *Arch Otolaryngol Head Neck Surg* 131(11):1007–1013